

Gradient boosting-based numerical methods for high-dimensional backward stochastic differential equations

LONG TENG,

Lehrstuhl für Angewandte Mathematik und Numerische Analysis,
Fakultät für Mathematik und Naturwissenschaften,
Bergische Universität Wuppertal, Gaußstr. 20, 42119 Wuppertal, Germany,
teng@math.uni-wuppertal.de

Abstract

In this work we propose a new algorithm for solving high-dimensional backward stochastic differential equations (BSDEs). Based on the general theta-discretization for the time-integrands, we show how to efficiently use eXtreme Gradient Boosting (XGBoost) regression to approximate the resulting conditional expectations in a quite high dimension. Numerical results illustrate the efficiency and accuracy of our proposed algorithms for solving very high-dimensional (up to 10000 dimensions) nonlinear BSDEs.

Keywords backward stochastic differential equations (BSDEs), XGBoost, high-dimensional problem, regression

MSC classes: 65M75, 60H35, 65C30

1 Introduction

It is well-known that the curse of dimensionality makes computation of partial differential equations (PDEs) and backward stochastic differential equations (BSDEs) challenging. In this paper we consider BSDEs of the form

$$\begin{cases} dX_t = a(t, X_t) dt + b(t, X_t) dW_t, & X_0 = x_0, \\ -dY_t = f(t, X_t, Y_t, Z_t) dt - Z_t dW_t, \\ Y_T = \xi = g(X_T), \end{cases} \quad (1)$$

where $a : [0, T] \times \mathbb{R}^d \rightarrow \mathbb{R}^d$, $b : [0, T] \times \mathbb{R}^d \rightarrow \mathbb{R}^{d \times d}$, $f(t, X_t, Y_t, Z_t) : [0, T] \times \mathbb{R}^d \times \mathbb{R} \times \mathbb{R}^d \rightarrow \mathbb{R}$ is the driver function and ξ is the square-integrable terminal condition. Many problems (e.g., pricing, hedging) in the field of finance and physics can be represented by such BSDEs, which makes problems easier to solve but exhibits usually no analytical solution, see e.g., [Karoui et al., 1997a]. Furthermore, the dimension d can be very high in applications, e.g., d is the number of underlying assets in financial applications. In the case of that f is linear, the solutions of high-dimensional problems can efficiently be approximated by the Monte-Carlo based approaches with the aid of the Feynman-Kac formula. Equation (1) becomes more challenging when f is nonlinear, and d is quite large (several hundreds), the classical approaches, such as finite difference methods, finite element methods, and nested Monte-Carlo methods suffer from the curse of dimensionality, i.e., their complexity grows exponentially in the dimension.

Recently, several approximation algorithms have been proposed to solve high-dimensional (≥ 100 *dim*) nonlinear BSDEs. The fully history recursive multilevel Picard approximation

(MLP) method has been proposed in [E. et al., 2019], and this method has been further studied in e.g., [Becker et al., 2020, Hutzenthaler and Kruse, 2020, Hutzenthaler et al., 2020] for solving high-dimensional PDEs. Another class of approximation algorithms are the deep learning-based approximation methods, for which we refer to [Beck et al., 2019b, Beck et al., 2019a, E. et al., 2017, Han et al., 2017, Ji et al., 2020, Kapllani and Teng, 2020]. Note that, for both the classes (the MLP and deep learning based method) above we only mention the references, in which the high dimensional nonlinear problems (≥ 100 dim) are dealt with and shown. There are also many other attempts in those classes in the literature to solve high-dimensional (up to 50 dim) BSDEs, for this we refer [Beck et al., 2020, Germain et al., 2021] for a nice overview.

The approximation algorithms in the references mentioned above are based on a reformulation, e.g., PDE as a suitable stochastic fixed point equation or stochastic control problem, and then with a forward discretization of the BSDE. For backward deep learning based approximation algorithms we refer to [Germain et al., 2020, Pham et al., 2021, Huré et al., 2020], in which 15, 20 and 50 dimensional numerical examples are considered, respectively. In [Teng, 2019], based on the backward theta-discretization for the time-integrands, the resulting conditional expectations are approximated using the regression tree, in which several 100 dimensional numerical experiments are shown. To approximate those conditional expectations on spatial discretization we refer to [Ruijter and Oosterlee, 2015] for the Fourier method, and e.g., [Teng et al., 2020, Teng and Zhao, 2021, Zhao et al., 2014] for the Gaussian quadrature rules.

In this paper, we propose gradient boosting-based backward approximation algorithms for solving high-dimensional nonlinear BSDEs. As in [Teng, 2019], we use the general theta-discretization method for the time-integrands and approximate the resulting conditional expectations using the eXtreme Gradient Boosting (XGBoost) regression [Chen and Guestrin, 2016]. Several numerical experiments of different types of high-dimensional problems are performed to demonstrate the efficiency and accuracy of our proposed algorithms.

In the next section, we start with notation and definitions and discuss in Section 3 the discretization of time-integrands using the theta-method, and derive the reference equations. Section 4 is devoted to how to use the XGBoost regression to approximate the conditional expectations. In Section 5, several numerical experiments on different types of quite high-dimensional BSDEs including financial applications are provided. Finally, Section 6 concludes this work.

2 Preliminaries

Throughout the paper, we assume that $(\Omega, \mathcal{F}, P; \{\mathcal{F}_t\}_{0 \leq t \leq T})$ is a complete, filtered probability space. In this space, a standard d -dimensional Brownian motion W_t with a finite terminal time T is defined, which generates the filtration $\{\mathcal{F}_t\}_{0 \leq t \leq T}$, i.e., $\mathcal{F}_t = \sigma\{W_s, 0 \leq s \leq t\}$ for BSDEs. And the usual hypotheses should be satisfied. We denote the set of all \mathcal{F}_t -adapted and square integrable processes in \mathbb{R}^d with $L^2 = L^2(0, T; \mathbb{R}^d)$. A pair of process (Y_t, Z_t) is the solution of the BSDEs (1) if it is \mathcal{F}_t -adapted and square integrable and satisfies (1) as

$$Y_t = \xi + \int_t^T f(s, X_s, Y_s, Z_s) ds - \int_t^T Z_s dW_s, \quad t \in [0, T], \quad (2)$$

where $f(t, X_s, Y_s, Z_s) : [0, T] \times \mathbb{R}^d \times \mathbb{R} \times \mathbb{R}^d \rightarrow \mathbb{R}$ is \mathcal{F}_t adapted, $\xi = g(X_T) : \mathbb{R}^d \rightarrow \mathbb{R}$. These solutions exist uniquely under Lipschitz conditions, see [Pardoux and Peng, 1990, Pardoux and Peng, 1992].

Suppose that the terminal value Y_T is of the form $g(X_T^{t,x})$, where $X_T^{t,x}$ denotes the solution of dX_t in (1) starting from x at time t . Then the solution $(Y_t^{t,x}, Z_t^{t,x})$ of BSDEs (1) can be represented

[Karoui et al., 1997b, Ma and Zhang, 2005, Pardoux and Peng, 1992, Peng, 1991] as

$$Y_t^{t,x} = u(t, x), \quad Z_t^{t,x} = b^\top(t, x)\nabla u(t, x) \quad \forall t \in [0, T],$$

which is solution of the semi-linear parabolic PDE of the form

$$\frac{\partial u}{\partial t} + \sum_i^n a_i \partial_i u + \frac{1}{2} \sum_{i,j}^n (bb^\top)_{i,j} \partial_{i,j}^2 u + f(t, x, u, (\nabla u)b) = 0$$

with the terminal condition $u(T, x) = g(x)$. In turn, suppose (Y, Z) is the solution of BSDEs, $u(t, x) = Y_t^{t,x}$ is a viscosity solution to the PDEs.

3 Discretization of the BSDE using theta-method

For simplicity, we discuss the discretization with one-dimensional processes, namely $d = 1$. And the extension to higher dimensions is possible and straightforward. We introduce the time partition for the time interval $[0, T]$

$$\Delta_t = \{t_i | t_i \in [0, T], i = 0, 1, \dots, N_T, t_i < t_{i+1}, t_0 = 0, t_{N_T} = T\}.$$

Let $\Delta t_i = t_{i+1} - t_i$ be the time step, and denote the maximum time step with Δt . One needs to additionally discretize the forward SDE in (1)

$$X_t = x_0 + \int_0^t a(s, X_s) ds + \int_0^t b(s, X_s) dW_s. \quad (3)$$

Suppose that the forward SDE (3) can be already discretized by a process $X_{t_i}^{\Delta t}$ such that

$$E \left[\max_{t_i} |X_{t_i} - X_{t_i}^{\Delta t}|^2 \right] = \mathcal{O}(\Delta t)$$

which means strong mean square convergence of order $1/2$. In the case of that X_t follows a known distribution (e.g., geometric Brownian motion), one can obtain good samples on Δt using the known distribution, otherwise the Euler scheme can be employed.

For the backward process (2), the well-known generalized θ -discretization for Z reads [Zhao et al., 2009, Zhao et al., 2012]

$$\begin{aligned} -E_i[Y_{i+1}\Delta W_{i+1}] &= \Delta t_i(1 - \theta_1)E_i[f(t_{i+1}, \mathbb{X}_{i+1})\Delta W_{i+1}] - \Delta t_i\theta_2 Z_i \\ &\quad - \Delta t_i(1 - \theta_2)E_i[Z_{i+1}] + R_\theta^{Z_i}, \end{aligned} \quad (4)$$

where $\theta_1 \in [0, 1], \theta_2 \in (0, 1]$ and $R_\theta^{Z_i}$ is the discretization error. Therefore, the equation (4) lead to a time discrete approximation $Z^{\Delta t}$ for Z

$$Z_i^{\Delta t} = \frac{\theta_2^{-1}}{\Delta t_i} E_i[Y_{i+1}^{\Delta t} \Delta W_{i+1}] + \theta_2^{-1}(1 - \theta_1)E_i[f(t_{i+1}, \mathbb{X}_{i+1}^{\Delta t})\Delta W_{i+1}] - \theta_2^{-1}(1 - \theta_2)E_i[Z_{i+1}^{\Delta t}]$$

And for Y one has

$$Y_i = E_i[Y_{i+1}] + \Delta t_i\theta_3 f(t_i, \mathbb{X}_i) + \Delta t_i(1 - \theta_3)E_i[f(t_{i+1}, \mathbb{X}_{i+1})] + R_\theta^{Y_i}, \quad \theta_3 \in [0, 1] \quad (5)$$

where $R_\theta^{Y_i}$ is the corresponding discretization error. Note that, due to $\mathbb{X}_i^{\Delta t} = (X_i^{\Delta t}, Y_i^{\Delta t}, Z_i^{\Delta t})$, (5) is implicit and can be solved by using iterative methods, e.g., Newton's method or Picard scheme.

By choosing the different values for θ_1 and θ_2 , one can obtain different schemes. For example, one receives the Crank-Nicolson scheme by setting $\theta_1 = \theta_2 = \theta_3 = 1/2$, which is second-order accurate. When $\theta_1 = \theta_2 = \theta_3 = 1$, the scheme is first-order accurate, see [Zhao et al., 2006, Zhao et al., 2009, Zhao et al., 2013]. Using the regression tree-based method in [Teng, 2019], the author focus on the scheme of $\theta_1 = 1/2, \theta_2 = 1, \theta_3 = 1/2$ for numerical examples. With the XGBoost regression in this paper, we suggest to use $\theta_1 = \theta_2 = \theta_3 = 1/2$ for a higher accuracy if g is continuously differentiable, i.e., Z_{N_T} is known analytically. ∇g denotes the gradient of g .

Semidiscrete Scheme 1

$$Y_{N_T}^{\Delta t} = g(X_{N_T}^{\Delta t}), Z_{N_T}^{\Delta t} = \nabla g(X_{N_T}^{\Delta t}), \quad (6)$$

For $i = N_T - 1, \dots, 0$:

$$Z_i^{\Delta t} = \frac{2}{\Delta t_i} E_i[Y_{i+1}^{\Delta t} \Delta W_{i+1}] + E_i[f(t_{i+1}, \mathbb{X}_{i+1}^{\Delta t}) \Delta W_{i+1}] - E_i[Z_{i+1}^{\Delta t}], \quad (7)$$

$$Y_i^{\Delta t} = E_i[Y_{i+1}^{\Delta t}] + \frac{\Delta t_i}{2} f(t_i, \mathbb{X}_i^{\Delta t}) + \frac{\Delta t_i}{2} E_i[f(t_{i+1}, \mathbb{X}_{i+1}^{\Delta t})], \quad (8)$$

Otherwise, the scheme $\theta_1 = \theta_2 = \theta_3 = 1$ should be used, in which Z_{N_T} is not needed to start the iteration, i.e.,

Semidiscrete Scheme 2

$$Y_{N_T}^{\Delta t} = g(X_{N_T}^{\Delta t}), \quad (9)$$

For $i = N_T - 1, \dots, 0$:

$$Z_i^{\Delta t} = \frac{1}{\Delta t_i} E_i[Y_{i+1}^{\Delta t} \Delta W_{i+1}], \quad (10)$$

$$Y_i^{\Delta t} = E_i[Y_{i+1}^{\Delta t}] + \Delta t_i f(t_i, \mathbb{X}_i^{\Delta t}). \quad (11)$$

The error estimates for the schemes above are given in Section 4.5. X_t can be sampled on the grid Δ_t based on the available distribution or by applying e.g., the Euler method.

4 Computation of conditional expectations with the XGBoost regression

Following the idea proposed in [Teng, 2019], in this section we firstly introduce how to use the XGBoost regression to approximate the conditional expectations included in the semi-discrete Scheme 1 and 2, and explain why we choose the XGBoost. We then analyze the time complexity and convergence of the proposed algorithms.

4.1 Non-parametric regression

We assume that $(X_i^{\Delta t})_{i=0, \dots, N_t}$ is Markovian. The conditional expectations included in Scheme 1 and 2 are all of the form $E[Y|X]$ for square integrable random variables X and Y . Therefore, we present the XGBoost regression approach based on the form $E[Y|X]$ throughout this section.

Suppose that the model in non-parametric regression reads

$$Y = \eta(X) + \epsilon, \quad (12)$$

where ϵ has a zero expectation and a constant variance, and is independent with X . Obviously, it can be thus implied that

$$E[Y|X = x] = \eta(x). \quad (13)$$

To approximate the conditional expectations, our goal in regression is to find an estimator of this function, $\hat{\eta}(x)$. By non-parametric regression, we are not assuming a particular form for η . Instead of, $\hat{\eta}$ is represented by a XGBoost regressor. Suppose we have a dataset, $(\hat{x}_{\mathcal{M}}, \hat{y}_{\mathcal{M}})$, $\mathcal{M} = 1, \dots, M$, for (X, Y) . We split the data into training and test sets, and fit the model, namely XGBoostregressor on the training data. The regressor can be used to determine (predict) $E[Y|X = x]$ for an arbitrary x , whose value is not necessarily equal to one of samples $\hat{x}_{\mathcal{M}}$.

As an example, we specify the procedure for (7), which can be rewritten as

$$Z_i^{\Delta t} = E \left[\frac{2}{\Delta t_i} Y_{i+1}^{\Delta t} \Delta W_{i+1} + f(t_{i+1}, \mathbb{X}_{i+1}^{\Delta t}) \Delta W_{i+1} - Z_{i+1}^{\Delta t} | X_i^{\Delta t} \right], \quad i = N_T - 1, \dots, 0. \quad (14)$$

And there exist deterministic functions $z_i^{\Delta t}(x)$ such that

$$Z_i^{\Delta t} = z_i^{\Delta t}(X_i^{\Delta t}). \quad (15)$$

Starting from the time T , we fit the regressor \hat{R}_z for the conditional expectation in (14) using the dataset $(\hat{x}_{N_T-1, \mathcal{M}}, \frac{2}{\Delta t_{N_T-1}} \hat{y}_{N_T, \mathcal{M}} \Delta \hat{w}_{N_T, \mathcal{M}} + \hat{f}_{N_T, \mathcal{M}} \Delta \hat{w}_{N_T, \mathcal{M}} - \hat{z}_{N_T})$. Thereby, the function

$$z_{N_T-1}^{\Delta t}(x) = E \left[\frac{2}{\Delta t_{N_T-1}} Y_{N_T}^{\Delta t} \Delta W_{N_T} + f(t_{N_T}, \mathbb{X}_{N_T}^{\Delta t}) \Delta W_{N_T} - Z_{N_T}^{\Delta t} | X_{N_T-1}^{\Delta t} = x \right], \quad (16)$$

is estimated and presented by the regressor, which can predict the dataset $\hat{z}_{N_T-1, \mathcal{M}}$ of the random variable $Z_{N_T-1}^{\Delta t}$ based on the dataset $\hat{x}_{N_T-1, \mathcal{M}}$, for $\mathcal{M} = 1, \dots, M$. Recursively, backward in time, the dataset $\hat{z}_{N_T-1, \mathcal{M}}$ (and also $\hat{y}_{N_T-1, \mathcal{M}}$) will be used to generate the dataset $\hat{z}_{N_T-2, \mathcal{M}}$ of the random variables $Z_{N_T-2}^{\Delta t}$ at the time t_{N_T-2} . At the initial time $t = 0$, we have a fix initial value x_0 for X , i.e., a constant dataset. Using the regressor fitted at time t_1 we predict the solution $Z_0^{\Delta t} = z_0^{\Delta t}(x_0)$. Following the same procedure to the conditional expectations in (8), one obtains implicitly $Y_0^{\Delta t}$.

4.2 The XGBoost regression

Recently, three third-party gradient boosting algorithms, including XGBoost, Light Gradient Boosting Machine (LightGBM) [Ke et al., 2017] and Categorical Boosting (CatBoost)[Dorogush et al., 2018] have been developed for classification or regression predictive modelling problems. These ensemble algorithms have been widely used due to their speed and performance. There are many comparisons among those three algorithms in terms of both speed and accuracy. The common outcome is that XGBoost works generally well, in particular in terms of model accuracy, but slower than other two algorithms, LightGBM has usually a highest speed, and the CatBoost performs well only when one has categorical variables in the data and tune them properly. In principle, all the three algorithms can be used for our purpose, the differences on results are caused by differences in the boosting algorithms. We want to do regression without categorical features, and find XGBoost performs better than LightGBM in terms

of model accuracy in our experiment with Example 3 (challenging example). Therefore, in this work, we focus on the XGBoost regression. In the sequel of this section we show how to use the XGBoost algorithm [Chen and Guestrin, 2016] for approximating the conditional expectations in semidiscrete Scheme 1 and 2 by taking (16) as an example.

We denote the predicted conditional expectation $E[\mathcal{Z}|X = \hat{x}_{i,\mathcal{M}}]$ using the XGBoost model fitted with the dataset of \mathcal{Z} with $E_i^{\hat{x}_{i,\mathcal{M}}}[\mathcal{Z}]$, $\mathcal{M} = 1, \dots, M$, M is the sample size. For (16), using the dataset (samples) of X_i (which are $\hat{x}_{i,\mathcal{M}}$) and the dataset of $\mathcal{Z}_{i+1} = \frac{2}{\Delta t_i} Y_{i+1}^{\Delta t} \Delta W_{i+1} + f(t_{N_T}, \mathbb{X}_{i+1}^{\Delta t}) \Delta W_{i+1} - Z_{i+1}^{\Delta t}$ (which are $\hat{\mathcal{Z}}_{i+1,\mathcal{M}} = \frac{2}{\Delta t_i} \hat{y}_{i+1,\mathcal{M}} \Delta \hat{w}_{i+1,\mathcal{M}} + \hat{f}_{i+1,\mathcal{M}} \Delta \hat{w}_{i+1,\mathcal{M}} - \hat{z}_{i+1}$) we train a XGBoost model. Then, $\hat{z}_{i,\mathcal{M}} := E_i^{\hat{x}_{i,\mathcal{M}}}[\mathcal{Z}_{i+1}]$ means the predicted value of $E[\mathcal{Z}_{i+1}|X = \hat{x}_{i,\mathcal{M}}]$ with that fitted XGBoost model for approximating $z_i^{\Delta t}(\hat{x}_{i,\mathcal{M}})$, see (15). Therefore, for the i -th step, we define

$$R_{\text{xgb}}^{Z_i} = \frac{1}{M} \sum_{\mathcal{M}=1}^M \left(\hat{z}_{i,\mathcal{M}} - z_i^{\Delta t}(\hat{x}_{i,\mathcal{M}}) \right)^2, \quad (17)$$

as the approximation error. Note that $\hat{\mathcal{Z}}_{i+1,\mathcal{M}} = z_i^{\Delta t}(\hat{x}_{i,\mathcal{M}}) + \epsilon_{i,\mathcal{M}}^z$, ϵ_i^z has zero expectation and a constant variance Var_i^z . Therefore, (17) can be reformulated as

$$R_{\text{xgb}}^{Z_i} = \frac{1}{M} \sum_{\mathcal{M}=1}^M \left(\epsilon_{i,\mathcal{M}}^z - \left(\hat{z}_{i,\mathcal{M}} - \hat{\mathcal{Z}}_{i+1,\mathcal{M}} \right) \right)^2 \quad (18)$$

$$\leq 2\text{Var}_i^z + \frac{2}{M} \sum_{\mathcal{M}=1}^M \left(\hat{z}_{i,\mathcal{M}} - \hat{\mathcal{Z}}_{i+1,\mathcal{M}} \right)^2, \quad (19)$$

where the second term refers to the XGBoost regression error which will be analyzed in the following.

Regularized learning objective For simplicity we shall focus on $d = 1$, the results can be straightforwardly extended to multidimensional cases. And for a simplified notation we omit the index of the time step, e.g., $\hat{x}_{\mathcal{M}}$ instead of $\hat{x}_{i,\mathcal{M}}$. Suppose that a given dataset with M samples

$$\mathcal{D} = \left\{ (\hat{x}_{\mathcal{M}}, \hat{\mathcal{Z}}_{\mathcal{M}}) \mid |\mathcal{D}| = M, \hat{x}_{\mathcal{M}}, \hat{\mathcal{Z}}_{\mathcal{M}} \in \mathbb{R} \right\}.$$

A tree ensemble model consists of K regression trees can be constructed to predict the output

$$\hat{z}_{\mathcal{M}} = \eta(\hat{x}_{\mathcal{M}}) = \sum_{k=1}^K \tilde{f}_k(\hat{x}_{\mathcal{M}}), \quad \tilde{f}_k \in \mathcal{S},$$

where $\mathcal{S} = \{ \tilde{f}(x) = \omega_{q(x)}, q : \mathbb{R} \rightarrow \hat{T}, \omega \in \mathbb{R}^{\hat{T}} \}$ is the space of regression trees. q denotes the structure of each tree that maps an example to the corresponding leaf index, i.e., each \tilde{f}_k corresponds to an independent tree structure q and leaf weights ω . ω_j represents score on the j -th leaf, and \hat{T} is the number of leaves.

To train the model we optimize the mean squared error (MSE) for regression

$$L(\hat{z}_{\mathcal{M}}, \hat{\mathcal{Z}}_{\mathcal{M}}) = \frac{1}{M} \sum_{\mathcal{M}=1}^M (\hat{z}_{\mathcal{M}} - \hat{\mathcal{Z}}_{\mathcal{M}})^2.$$

For a regularized objective we define the regularization term

$$\Omega(\tilde{f}) = \gamma \hat{T} + \frac{1}{2} \lambda \|w\|^2 = \gamma \hat{T} + \frac{1}{2} \lambda \sum_{j=1}^{\hat{T}} w_j^2,$$

where γ, λ are positive regularization parameter, and w_j is the score on the j -th leaf. The regularization term controls the complexity of the model which avoids overfitting. Therefore, the regularized objective is given by

$$\mathcal{L}(\eta) = \sum_{\mathcal{M}=1}^M L(\hat{z}_{\mathcal{M}}, \hat{\mathcal{Z}}_{\mathcal{M}}) + \sum_{k=1}^K \Omega(f_k), \quad (20)$$

which needs to be minimized, L serves as a loss function that measures the difference between the prediction and target.

Gradient Tree Boosting In XGBoost, the gradient descent is used to minimize (20), according to which we minimize the following objective by adding \tilde{f}_k in a iterative algorithm

$$\mathcal{L}^{(k)} = \sum_{\mathcal{M}=1}^M L(\hat{\mathcal{Z}}_{\mathcal{M}}, \hat{z}_{\mathcal{M}}^k) + \sum_{j=1}^k \Omega(\tilde{f}_j) = \sum_{\mathcal{M}=1}^M L(\hat{\mathcal{Z}}_{\mathcal{M}}, \hat{z}_{\mathcal{M}}^{(k-1)} + \tilde{f}_k(\hat{x}_{\mathcal{Z}})) + \Omega(\tilde{f}_k), \quad (21)$$

where $\hat{z}_{\mathcal{M}}^k = \sum_{j=1}^k \tilde{f}_j(\mathbf{x}_{\mathcal{M}})$, and $k = 1, \dots, K$. This is to say that (20) is minimized by greedily adding \tilde{f}_k . For this, one calculates a second-order approximation of (21) as

$$\mathcal{L}^{(k)} \approx \sum_{\mathcal{M}=1}^M \left(L(\hat{\mathcal{Z}}_{\mathcal{M}}, \hat{z}_{\mathcal{M}}^{(k-1)}) + g_{\mathcal{M}} \tilde{f}_k(\hat{x}_{\mathcal{M}}) + \frac{1}{2} h_{\mathcal{M}} \tilde{f}_k^2(\hat{x}_{\mathcal{M}}) \right) + \Omega(\tilde{f}_k),$$

where $g_{\mathcal{M}} = \partial_{\hat{z}_{\mathcal{M}}^{(k-1)}} L(\hat{\mathcal{Z}}_{\mathcal{M}}, \hat{z}_{\mathcal{M}}^{(k-1)})$ and $h_{\mathcal{M}} = \partial_{\hat{z}_{\mathcal{M}}^{(k-1)}}^2 L(\hat{\mathcal{Z}}_{\mathcal{M}}, \hat{z}_{\mathcal{M}}^{(k-1)})$ are first and second order gradients, respectively. By removing the constant terms one obtains the objective at k -th step

$$\tilde{\mathcal{L}}^{(k)} = \sum_{\mathcal{M}=1}^M \left(g_{\mathcal{M}} \tilde{f}_k(\hat{x}_{\mathcal{M}}) + \frac{1}{2} h_{\mathcal{M}} \tilde{f}_k^2(\hat{x}_{\mathcal{M}}) \right) + \Omega(\tilde{f}_k), \quad (22)$$

which needs to be optimized by finding a \tilde{f}_k .

Next, we show how can one find the tree \tilde{f}_k to optimize the prediction. We firstly define a tree as

$$\tilde{f}_k(\hat{x}) = w_{q(\hat{x})}, \quad w \in \mathbb{R}^{\hat{T}}.$$

And define $I_j = \{\mathcal{M} | q(\hat{x}_{\mathcal{M}}) = j\}$ as the instance set of leaf j , which contains the indices of data points mapped to the j -th leaf. Then, (22) can be rewritten as

$$\begin{aligned} \tilde{\mathcal{L}}^{(k)} &= \sum_{\mathcal{M}=1}^M \left(g_{\mathcal{M}} \tilde{f}_k(\hat{x}_{\mathcal{M}}) + \frac{1}{2} h_{\mathcal{M}} \tilde{f}_k^2(\hat{x}_{\mathcal{M}}) \right) + \gamma \hat{T} + \frac{1}{2} \lambda \sum_{j=1}^{\hat{T}} w_j^2 \\ &= \sum_{j=1}^{\hat{T}} \left(\left(\sum_{\mathcal{M} \in I_j} g_{\mathcal{M}} \right) w_j + \frac{1}{2} \left(\sum_{\mathcal{M} \in I_j} h_{\mathcal{M}} + \lambda \right) w_j^2 \right) + \gamma \hat{T}. \end{aligned}$$

For a fixed $q(\hat{x})$, one can easily compute the optimal w_j of leaf j as

$$w_j^* = - \frac{\sum_{\mathcal{M} \in I_j} g_{\mathcal{M}}}{\sum_{\mathcal{M} \in I_j} h_{\mathcal{M}} + \lambda},$$

and thus the corresponding optimal value of the objective

$$\tilde{\mathcal{L}}^{(k)}(q) = - \frac{1}{2} \sum_{j=1}^{\hat{T}} \frac{(\sum_{\mathcal{M} \in I_j} g_{\mathcal{M}})^2}{\sum_{\mathcal{M} \in I_j} h_{\mathcal{M}} + \lambda} + \gamma \hat{T}, \quad (23)$$

which can be used as a scoring function to measure the quality of q . Due to the high computational cost, it is not realistic to enumerate all the possible q . A greedy algorithm proposed in [Chen and Guestrin, 2016] that finds best splitting point recursively until the maximum depth. We denote the instance sets of left and right nodes after the split by I_L and I_R , and $I = I_L \cup I_R$. The following loss reduction after the split

$$\mathcal{L}_{\text{gain}} = \frac{1}{2} \left(\frac{(\sum_{\mathcal{M} \in I_L} g_{\mathcal{M}})^2}{\sum_{\mathcal{M} \in I_L} h_{\mathcal{M}} + \lambda} + \frac{(\sum_{\mathcal{M} \in I_R} g_{\mathcal{M}})^2}{\sum_{\mathcal{M} \in I_R} h_{\mathcal{M}} + \lambda} - \frac{(\sum_{\mathcal{M} \in I} g_{\mathcal{M}})^2}{\sum_{\mathcal{M} \in I} h_{\mathcal{M}} + \lambda} \right) - \gamma \quad (24)$$

is used for evaluating the split candidates, where λ is the regularization parameter. Based on the best splitting point, one can then prune out the nodes with a negative gain.

We have introduced the mathematics behind XGBoost. For all other techniques used in the implementation to further prevent overfitting (shrinkage [Friedman, 2002], column feature sub-sampling [Breiman, 2001, Friedman and Popescu, 2003]), improve the efficiency (approximate exact greedy algorithm, sparsity-aware splitting, column block for parallel learning) we refer to [Chen and Guestrin, 2016].

4.3 The fully discrete schemes

In this section we introduce the fully discrete schemes, where the conditional expectations approximated by XGBoost regression. As shown above, we do not need regression for each conditional expectation in semidiscrete Scheme 1 and 2. Due to the linearity of conditional expectation, we perform XGBoost regression for the combination of the conditional expectations in one equation. Based on semidiscrete Scheme 1, by combining conditional expectations and including all errors we give the following fully discrete scheme 1 as:

Fully discrete Scheme 1

$$\hat{y}_{N_T, \mathcal{M}} = g(\hat{x}_{N_T, \mathcal{M}}), \hat{z}_{N_T, \mathcal{M}} = g_x(\hat{x}_{N_T, \mathcal{M}}),$$

For $i = N_T - 1, \dots, 0$, $\mathcal{M} = 1, \dots, M$:

$$\hat{z}_{i, \mathcal{M}} = E_i^{\hat{x}_{i, \mathcal{M}}} \left[\frac{2}{\Delta t_i} Y_{i+1} \Delta W_{i+1} + f(t_{i+1}, \mathbb{X}_{i+1}) \Delta W_{i+1} - Z_{i+1} \right], \quad (25)$$

$$\hat{y}_{i, \mathcal{M}} = E_i^{\hat{x}_{i, \mathcal{M}}} \left[Y_{i+1} + \frac{\Delta t_i}{2} f(t_{i+1}, \mathbb{X}_{i+1}) \right] + \frac{\Delta t_i}{2} \hat{f}_{i, \mathcal{M}}. \quad (26)$$

The error of approximating conditional expectations by using the XGBoost regression in (25), namely $R_{\text{xgb}}^{Z_i}$ is given in (17) and bounded by $2(\text{Var}_i^z + \hat{\mathcal{L}}_{\min}(\hat{q}_i^z))$, where $\hat{\mathcal{L}}_{\min}(\hat{q}_i^z)$ is defined via (23). \hat{q}_i^z denotes representation of the tree structure with the smallest error at i -th step. Similarly, for the regression error in (26) we define

$$R_{\text{xgb}}^Y = \frac{1}{M} \sum_{\mathcal{M}=1}^M \left(\hat{y}_{i, \mathcal{M}} - y_i^{\Delta t}(\hat{x}_{i, \mathcal{M}}) \right)^2 \leq 2(\text{Var}_i^y + \hat{\mathcal{L}}_{\min}(\hat{q}_i^y)). \quad (27)$$

Analogously, the fully discrete scheme 2 can be given as:

$$\begin{aligned}\hat{y}_{N_T, \mathcal{M}} &= g(\hat{x}_{N_T, \mathcal{M}}), \\ \text{For } i &= N_T - 1, \dots, 0, \mathcal{M} = 1, \dots, M : \\ \hat{z}_{i, \mathcal{M}} &= E_i^{\hat{x}_{i, \mathcal{M}}} \left[\frac{1}{\Delta t_i} Y_{i+1} \Delta W_{i+1} \right], \\ \hat{y}_{i, \mathcal{M}} &= E_i^{\hat{x}_{i, \mathcal{M}}} [Y_{i+1}] + \Delta t_i \hat{f}_{i, \mathcal{M}}.\end{aligned}$$

4.4 Time complexity analysis

We denote the maximum depth of the tree by \tilde{d} , and the total number of trees by K . The time complexity of the XGBoost reads [Chen and Guestrin, 2016]

$$\mathcal{O}(K\tilde{d}|\text{samples}| + |\text{samples}| \log B), \quad (28)$$

where $|\text{samples}|$ denotes number of samples in the training data, and B is the maximum number of rows in each block. Note that $\mathcal{O}(|\text{samples}| \log B)$ is the one time preprocessing cost. From (28) we straightforwardly deduce that the complexity of approximating one conditional expectation in our scheme is $\mathcal{O}(K\tilde{d}Md + Md \log B)$. Therefore, the time complexity of our proposed scheme is given by

$$\mathcal{O}(K\tilde{d}MdN_T + MdN_T \log B).$$

4.5 Error estimates

The error analysis when $\theta_1 = 1/2, \theta_2 = 1, \theta_3 = 1/2$ has been done in [Teng, 2019], we generalize it for the general theta-scheme, i.e., which includes the proposed Scheme 1 and 2. Suppose that the errors of iterative method can be neglected by choosing the number of Picard iterations sufficiently high, we consider the discretization and regression errors in the first place. The errors due to the time-discretization are given by

$$\begin{aligned}\epsilon^{Y_i, \theta} &:= Y_i - Y_i^{\Delta t}, \\ \epsilon^{Z_i, \theta} &:= Z_i - Z_i^{\Delta t}, \\ \epsilon^{f_i, \theta} &:= f(t_i, \mathbb{X}_i) - f(t_i, \mathbb{X}_i^{\Delta t}).\end{aligned}$$

As the deterministic function $z_i^{\Delta t}$ given in (15) we define deterministic function $y_i^{\Delta t}$

$$Y_i^{\Delta t} = y_i^{\Delta t}(X_i^{\Delta t}).$$

These functions are approximated by the regression trees, resulting in the approximations $\hat{y}_i^{\Delta t}, \hat{z}_i^{\Delta t}$ with

$$\hat{Y}_i^{\Delta t} = \hat{y}_i^{\Delta t}(X_i^{\Delta t}) \text{ and } \hat{Z}_i^{\Delta t} = \hat{z}_i^{\Delta t}(X_i^{\Delta t}),$$

Thus, we denote the global errors by

$$\begin{aligned}\epsilon^{Y_i} &:= Y_i - \hat{Y}_i^{\Delta t}, \\ \epsilon^{Z_i} &:= Z_i - \hat{Z}_i^{\Delta t}, \\ \epsilon^{f_i} &:= f(t_i, \mathbb{X}_i) - f(t_i, \hat{\mathbb{X}}_i^{\Delta t}).\end{aligned}$$

Assumption 1 Suppose that X_0 is \mathcal{F}_0 -measurable with $E[|X_0|^2] < \infty$, and that a and b are L^2 -measurable in $(t, x) \in [0, T] \times \mathbb{R}^d$, are linear growth bounded and uniformly Lipschitz continuous, i.e., there exist positive constants K and L such that

$$\begin{aligned} |a(t, x)|^2 &\leq K(1 + |x|^2), & |b(t, x)|^2 &\leq K(1 + |x|^2), \\ |a(t, x) - a(t, y)| &\leq L|x - y|, & |b(t, x) - b(t, y)| &\leq L|x - y| \end{aligned}$$

with $x, y \in \mathbb{R}^d$.

Let $C_b^{l,k,k,k}$ be the set of continuously differentiable functions $f : [0, T] \times \mathbb{R}^n \times \mathbb{R}^m \times \mathbb{R}^{m \times d} \rightarrow \mathbb{R}^m$ with uniformly bounded partial derivatives $\partial_t^{l_1} f$ for $\frac{1}{2} \leq l_1 \leq l$ and $\partial_x^{k_1} \partial_y^{k_2} \partial_z^{k_3} f$ for $1 \leq k_1 + k_2 + k_3 \leq k$, $C_b^{l,k,k}$ and $C_b^{l,k}$ can be analogously defined, and C_b^k be the set of functions $g : \mathbb{R}^d \rightarrow \mathbb{R}^m$ with uniformly bounded partial derivatives $\partial_x^{k_1} g$ for $1 \leq k_1 \leq k$. We give some remarks concerning related results on the one-step scheme:

- Under Assumption 4.1, if $f \in C_b^{2,4,4,4}$, $g \in C_b^{4+\alpha}$ for some $\alpha \in (0, 1)$, a and b are bounded, and $a, b \in C_b^{2,4}$, the absolute values of the local errors $R_\theta^{Y_i}$ and $R_\theta^{Z_i}$ can be bounded by $C(\Delta t_i)^3$ in Scheme 1 and by $C(\Delta t_i)^2$ in Scheme 2, where C is a constant which can depend on T, x_0 and the bounds of a, b, f, g in (1), see e.g., [Yang et al., 2017, Zhao et al., 2009, Zhao et al., 2014, Zhao et al., 2012, Zhao et al., 2013].
- For notation convenience we might omit the dependency of local and global errors on state of the BSDEs and the discretization errors of dX_t , namely we assume that $X_i = X_i^{\Delta t}$. And we focus on 1-dimensional case ($d = 1$), the results can be extended to high-dimensional case.
- For the implicit schemes we will apply Picard iterations which converges because of the Lipschitz assumptions on the driver, and for any initial guess when Δt_i is small enough. In the following analysis, we consider the equidistant time discretization Δt .

For the Z -component ($0 \leq i \leq N_T - 1$) we have (see (4))

$$\epsilon^{Z_i} = E_i^{x_i} \left[\frac{1}{\Delta t \theta_2} \epsilon^{Y_{i+1}} \Delta W_{i+1} + \frac{1 - \theta_1}{\theta_2} \epsilon^{f_{i+1}} \Delta W_{i+1} - \frac{1 - \theta_2}{\theta_2} \epsilon^{Z_{i+1}} \right] + \frac{R_\theta^{Z_i}}{\Delta t \theta_2} + R_{\text{rgb}}^{Z_i},$$

where the $\epsilon^{f_{i+1}}$ can be bounded using Lipschitz continuity of f by

$$E_i^{x_i} [|\epsilon^{f_{i+1}}|^2] \leq E_i^{x_i} [L(|\epsilon^{Y_{i+1}}| + |\epsilon^{Z_{i+1}}|)^2] \leq 2L^2 E_i^{x_i} [|\epsilon^{Y_{i+1}}|^2 + |\epsilon^{Z_{i+1}}|^2]$$

with Lipschitz constant L . And it holds that

$$|E_i^{x_i} [\epsilon^{Y_{i+1}} \Delta W_{i+1}]|^2 = |E_i^{x_i} [(\epsilon^{Y_{i+1}} - E_i^{x_i}[\epsilon^{Y_{i+1}}]) \Delta W_{i+1}]|^2 \leq \Delta t (E_i^{x_i} [|\epsilon^{Y_{i+1}}|^2] - |E_i^{x_i}[\epsilon^{Y_{i+1}}]|^2)$$

with Cauchy-Schwarz inequality. Consequently, we calculate

$$\begin{aligned} \theta_2^2 (\Delta t)^2 |\epsilon^{Z_i}|^2 &\leq 2\Delta t (E_i^{x_i} [|\epsilon^{Y_{i+1}}|^2] - |E_i^{x_i}[\epsilon^{Y_{i+1}}]|^2) + 16(1 - \theta_1)^2 L^2 (\Delta t)^3 E_i^{x_i} [|\epsilon^{Y_{i+1}}|^2 + |\epsilon^{Z_{i+1}}|^2] \\ &\quad + 8(\theta_2 - 1)^2 (\Delta t)^2 E_i^{x_i} [|\epsilon^{Z_{i+1}}|^2] + 8|R_\theta^{Z_i}|^2 + 8(\Delta t)^2 \theta_2^2 |R_{\text{rgb}}^{Z_i}|^2, \end{aligned} \tag{29}$$

where Hölder's inequality is used.

For the Y -component in the implicit scheme we have

$$\epsilon^{Y_i} = E_i^{x_i} [\epsilon^{Y_{i+1}} + (1 - \theta_3) \Delta t \epsilon^{f_{i+1}}] + \theta_3 \Delta t \epsilon^{f_i} + R_\theta^{Y_i} + R_{\text{rgb}}^{Y_i}.$$

This error can be bounded by

$$|\epsilon^{Y_i}| \leq |E_i^{x_i}[\epsilon^{Y_{i+1}}]| + \theta_3 \Delta t L (|\epsilon^{Y_i}| + |\epsilon^{Z_i}|) + (1 - \theta_3) \Delta t L E_i^{x_i} [|\epsilon^{Y_{i+1}}| + |\epsilon^{Z_{i+1}}|] + |R_\theta^{Y_i}| + |R_{\text{xgb}}^{Y_i}|.$$

By the inequality $(a + b)^2 \leq a^2 + b^2 + \gamma \Delta t a^2 + \frac{1}{\gamma \Delta t} b^2$ we calculate

$$\begin{aligned} |\epsilon^{Y_i}|^2 &\leq (1 + \gamma \Delta t) |E_i^{x_i}[\epsilon^{Y_{i+1}}]|^2 + 6\theta_3^2 (\Delta t L)^2 (|\epsilon^{Y_i}|^2 + |\epsilon^{Z_i}|^2) \\ &\quad + 6(1 - \theta_3)^2 (\Delta t L)^2 (E_i^{x_i} [|\epsilon^{Y_{i+1}}|^2] + E_i^{x_i} [|\epsilon^{Z_{i+1}}|^2]) + 6|R_\theta^{Y_i}|^2 + 6|R_{\text{xgb}}^{Y_i}|^2 \\ &\quad + \frac{1}{\gamma} (6\theta_3^2 \Delta t L^2 (|\epsilon^{Y_i}|^2 + |\epsilon^{Z_i}|^2) + 6(1 - \theta_3)^2 \Delta t L^2 (E_i^{x_i} [|\epsilon^{Y_{i+1}}|^2] + E_i^{x_i} [|\epsilon^{Z_{i+1}}|^2])) \\ &\quad + \frac{6|R_\theta^{Y_i}|^2}{\Delta t} + \frac{6|R_{\text{xgb}}^{Y_i}|^2}{\Delta t} \Big). \end{aligned} \quad (30)$$

Theorem 4.1. Under Assumption 4.1, if $f \in C_b^{2,4,4,4}$, $g \in C_b^{4+\alpha}$ for some $\alpha \in (0, 1)$, a and b are bounded, $a, b \in C_b^{2,4}$, and given

$$E_{N_T-1}^{x_{N_T-1}} [|\epsilon^{Z_{N_T}}|^2] \sim \mathcal{O}((\Delta t)^2), \quad E_{N_T-1}^{x_{N_T-1}} [|\epsilon^{Y_{N_T}}|^2] \sim \mathcal{O}((\Delta t)^2),$$

It holds then

$$E_0^{x_0} \left[|\epsilon^{Y_i}|^2 + \frac{(8\theta_3^2(\theta_2 - 1)^2 + (1 - \theta_3)^2 \theta_2^2) \Delta t}{2(1 - \theta_3)^2 + 2\theta_3^2} |\epsilon^{Z_i}|^2 \right] \leq Q(\Delta t)^2 + \tilde{Q} \sum_{i+1}^{N_T} \left(\frac{N_T (\text{Var}_j^Y)^2}{T} + \frac{T (\text{Var}_j^Z)^2}{N_T} \right), \quad (31)$$

$0 \leq i \leq N_T - 1$, where Q is a constant which only depend on T , x_0 and the bounds of f, g and a, b in (1), \tilde{Q} is a constant depending on T , x_0 and L , and Var_i^Y and Var_i^Z are the bounded constants, and M is the number of samples.

Proof. By combining both (29) and (30) we straightforwardly obtain

$$\begin{aligned} E_i^{x_i} [|\epsilon^{Y_i}|^2] + \frac{\theta_2^2 \Delta t}{2} E_i^{x_i} [|\epsilon^{Z_i}|^2] &\leq (1 + \gamma \Delta t) |E_i^{x_i}[\epsilon^{Y_{i+1}}]|^2 + 6\theta_3^2 (\Delta t L)^2 (E_i^{x_i} [|\epsilon^{Y_i}|^2] + E_i^{x_i} [|\epsilon^{Z_i}|^2]) \\ &\quad + 6(1 - \theta_3)^2 (\Delta t L)^2 (E_i^{x_i} [|\epsilon^{Y_{i+1}}|^2] + E_i^{x_i} [|\epsilon^{Z_{i+1}}|^2]) + 6E_i^{x_i} [|R_\theta^{Y_i}|^2] + 6E_i^{x_i} [|R_{\text{xgb}}^{Y_i}|^2] \\ &\quad + (E_i^{x_i} [|\epsilon^{Y_{i+1}}|^2] - |E_i^{x_i}[\epsilon^{Y_{i+1}}]|^2) + 8(1 - \theta_1)^2 (\Delta t L)^2 (E_i^{x_i} [|\epsilon^{Y_{i+1}}|^2] + E_i^{x_i} [|\epsilon^{Z_{i+1}}|^2]) \\ &\quad + 4(\theta_2 - 1)^2 \Delta t E_i^{x_i} [|\epsilon^{Z_{i+1}}|^2] + 4 \frac{E_i^{x_i} [|R_\theta^{Z_i}|^2]}{\Delta t} + 4\Delta t \theta_2^2 E_i^{x_i} [|R_{\text{xgb}}^{Z_i}|^2] \\ &\quad + \frac{1}{\gamma} (6\theta_3^2 \Delta t L^2 (E_i^{x_i} [|\epsilon^{Y_i}|^2] + E_i^{x_i} [|\epsilon^{Z_i}|^2]) + 6(1 - \theta_3)^2 \Delta t L^2 (E_i^{x_i} [|\epsilon^{Y_{i+1}}|^2] + E_i^{x_i} [|\epsilon^{Z_{i+1}}|^2])) \\ &\quad + \frac{6E_i^{x_i} [|R_\theta^{Y_i}|^2]}{\Delta t} + \frac{6E_i^{x_i} [|R_{\text{xgb}}^{Y_i}|^2]}{\Delta t} \Big) \end{aligned}$$

which implies

$$\begin{aligned} &\left(1 - 6\theta_3^2 (\Delta t L)^2 - \frac{6\theta_3^2 \Delta t L^2}{\gamma} \right) E_i^{x_i} [|\epsilon^{Y_i}|^2] + \left(\frac{\theta_2^2 \Delta t}{2} - 6\theta_3^2 (\Delta t L)^2 - \frac{6\theta_3^2 \Delta t L^2}{\gamma} \right) E_i^{x_i} [|\epsilon^{Z_i}|^2] \\ &\leq \left(1 + \gamma \Delta t + 6(1 - \theta_3)^2 (\Delta t L)^2 + 8(1 - \theta_1)^2 (\Delta t L)^2 + \frac{6(1 - \theta_3)^2 \Delta t L^2}{\gamma} \right) E_i^{x_i} [|\epsilon^{Y_{i+1}}|^2] \\ &\quad + \left(6(1 - \theta_3)^2 (\Delta t L)^2 + 8(1 - \theta_1)^2 (\Delta t L)^2 + 4(\theta_2 - 1)^2 \Delta t + \frac{6(1 - \theta_3)^2 \Delta t L^2}{\gamma} \right) E_i^{x_i} [|\epsilon^{Z_{i+1}}|^2] \\ &\quad + 6E_i^{x_i} [|R_\theta^{Y_i}|^2] + 6E_i^{x_i} [|R_{\text{xgb}}^{Y_i}|^2] + \frac{6E_i^{x_i} [|R_\theta^{Y_i}|^2]}{\gamma \Delta t} + \frac{6E_i^{x_i} [|R_{\text{xgb}}^{Y_i}|^2]}{\gamma \Delta t} + \frac{4E_i^{x_i} [|R_\theta^{Z_i}|^2]}{\Delta t} + 4\Delta t \theta_2^2 E_i^{x_i} [|R_{\text{xgb}}^{Z_i}|^2]. \end{aligned}$$

We choose γ such that $\frac{\theta_2^2 \Delta t}{2} - \frac{6\theta_3^2 \Delta t L^2}{\gamma} \geq 4(\theta_2 - 1)^2 \Delta t + \frac{6(1-\theta_3)^2 \Delta t L^2}{\gamma}$, *i.e.* $\gamma \geq \frac{12\theta_3^2 L^2 + 12(1-\theta_3)^2 L^2}{\theta_2^2 - 8(\theta_2 - 1)^2}$, by which the latter inequality can be rewritten as

$$\begin{aligned}
& \left(1 - 6\theta_3^2 (\Delta t L)^2 - \frac{\theta_3^2 \Delta t (\theta_2^2 - 8(\theta_2 - 1)^2)}{2\theta_3^2 + 2(1 - \theta_3)^2} \right) E_i^{x_i} [|\epsilon^{Y_i}|^2] \\
& + \left(\frac{(8\theta_3^2 (\theta_2 - 1)^2 + (1 - \theta_3)^2 \theta_2^2) \Delta t}{2(1 - \theta_3)^2 + 2\theta_3^2} - 6\theta_3^2 (\Delta t L)^2 \right) E_i^{x_i} [|\epsilon^{Z_i}|^2] \\
& \leq \left(1 + \frac{12\theta_3^2 L^2 + 12(1 - \theta_3)^2 L^2}{\theta_2^2 - 8(\theta_2 - 1)^2} \Delta t + 6(1 - \theta_3)^2 (\Delta t L)^2 + 8(1 - \theta_1)^2 (\Delta t L)^2 \right. \\
& + \left. \frac{(1 - \theta_3)^2 \Delta t (\theta_2^2 - 8(\theta_2 - 1)^2)}{2\theta_3^2 + 2(1 - \theta_3)^2} \right) E_i^{x_i} [|\epsilon^{Y_{i+1}}|^2] \\
& + \left(\frac{(8\theta_3^2 (\theta_2 - 1)^2 + (1 - \theta_3)^2 \theta_2^2) \Delta t}{2(1 - \theta_3)^2 + 2\theta_3^2} + 6(1 - \theta_3)^2 (\Delta t L)^2 + 8(1 - \theta_1)^2 (\Delta t L)^2 \right) E_i^{x_i} [|\epsilon^{Z_{i+1}}|^2] \\
& + 6E_i^{x_i} [|\epsilon^{R_\theta^{Y_i}}|^2] + 6E_i^{x_i} [|\epsilon^{R_{\text{rgb}}^{Y_i}}|^2] + \frac{(\theta_2^2 - 8(\theta_2 - 1)^2) E_i^{x_i} [|\epsilon^{R_\theta^{Y_i}}|^2]}{L^2 (2\theta_3^2 + 2(1 - \theta_3)^2) \Delta t} \\
& + \frac{(\theta_2^2 - 8(\theta_2 - 1)^2) E_i^{x_i} [|\epsilon^{R_{\text{rgb}}^{Y_i}}|^2]}{L^2 (2\theta_3^2 + 2(1 - \theta_3)^2) \Delta t} + \frac{4E_i^{x_i} [|\epsilon^{R_\theta^{Z_i}}|^2]}{\Delta t} + 4\Delta t \theta_2^2 E_i^{x_i} [|\epsilon^{R_{\text{rgb}}^{Z_i}}|^2].
\end{aligned}$$

which implies

$$\begin{aligned}
& E_i^{x_i} [|\epsilon^{Y_i}|^2] + \frac{(8\theta_3^2 (\theta_2 - 1)^2 + (1 - \theta_3)^2 \theta_2^2) \Delta t}{2(1 - \theta_3)^2 + 2\theta_3^2} E_i^{x_i} [|\epsilon^{Z_i}|^2] \leq \frac{1 + C\Delta t}{1 - C\Delta t} \left((E_i^{x_i} [|\epsilon^{Y_{i+1}}|^2] \right. \\
& + \left. \frac{(8\theta_3^2 (\theta_2 - 1)^2 + (1 - \theta_3)^2 \theta_2^2) \Delta t}{2(1 - \theta_3)^2 + 2\theta_3^2} E_i^{x_i} [|\epsilon^{Z_{i+1}}|^2] \right) + 6E_i^{x_i} [|\epsilon^{R_\theta^{Y_i}}|^2] + 6E_i^{x_i} [|\epsilon^{R_{\text{rgb}}^{Y_i}}|^2] \\
& + \left. \frac{(\theta_2^2 - 8(\theta_2 - 1)^2) E_i^{x_i} [|\epsilon^{R_\theta^{Y_i}}|^2]}{L^2 (2\theta_3^2 + 2(1 - \theta_3)^2) \Delta t} + \frac{(\theta_2^2 - 8(\theta_2 - 1)^2) E_i^{x_i} [|\epsilon^{R_{\text{rgb}}^{Y_i}}|^2]}{L^2 (2\theta_3^2 + 2(1 - \theta_3)^2) \Delta t} + \frac{4E_i^{x_i} [|\epsilon^{R_\theta^{Z_i}}|^2]}{\Delta t} + 4\Delta t \theta_2^2 E_i^{x_i} [|\epsilon^{R_{\text{rgb}}^{Z_i}}|^2] \right).
\end{aligned}$$

By induction, we obtain then

$$\begin{aligned}
& E_i^{x_i} [|\epsilon^{Y_i}|^2] + \frac{(8\theta_3^2 (\theta_2 - 1)^2 + (1 - \theta_3)^2 \theta_2^2) \Delta t}{2(1 - \theta_3)^2 + 2\theta_3^2} E_i^{x_i} [|\epsilon^{Z_i}|^2] \leq \left(\frac{1 + C\Delta t}{1 - C\Delta t} \right)^{N_T - i} \left(E_{N_T - 1}^{x_{N_T - 1}} [|\epsilon^{Y_{N_T}}|^2] \right. \\
& + \left. \frac{(8\theta_3^2 (\theta_2 - 1)^2 + (1 - \theta_3)^2 \theta_2^2) \Delta t}{2(1 - \theta_3)^2 + 2\theta_3^2} E_{N_T - 1}^{x_{N_T - 1}} [|\epsilon^{Z_{N_T}}|^2] \right) \\
& + \sum_{j=i+1}^{N_T} \left(\frac{1 + C\Delta t}{1 - C\Delta t} \right)^{j-i} \left(6E_i^{x_i} [|\epsilon^{R_\theta^{Y_j}}|^2] + 6E_i^{x_i} [|\epsilon^{R_{\text{rgb}}^{Y_j}}|^2] + \frac{(\theta_2^2 - 8(\theta_2 - 1)^2) E_i^{x_i} [|\epsilon^{R_\theta^{Y_j}}|^2]}{L^2 (2\theta_3^2 + 2(1 - \theta_3)^2) \Delta t} \right. \\
& + \left. \frac{(\theta_2^2 - 8(\theta_2 - 1)^2) E_i^{x_i} [|\epsilon^{R_{\text{rgb}}^{Y_j}}|^2]}{L^2 (2\theta_3^2 + 2(1 - \theta_3)^2) \Delta t} + \frac{4E_i^{x_i} [|\epsilon^{R_\theta^{Z_j}}|^2]}{\Delta t} + 4\Delta t \theta_2^2 E_i^{x_i} [|\epsilon^{R_{\text{rgb}}^{Z_j}}|^2] \right) \\
& \leq \exp(2CT) \left(E_{N_T - 1}^{x_{N_T - 1}} [|\epsilon^{Y_{N_T}}|^2] + \frac{(8\theta_3^2 (\theta_2 - 1)^2 + (1 - \theta_3)^2 \theta_2^2) \Delta t}{2(1 - \theta_3)^2 + 2\theta_3^2} E_{N_T - 1}^{x_{N_T - 1}} [|\epsilon^{Z_{N_T}}|^2] \right) \\
& + \exp(2CT) \sum_{j=i+1}^{N_T} \left(6E_i^{x_i} [|\epsilon^{R_\theta^{Y_j}}|^2] + 6E_i^{x_i} [|\epsilon^{R_{\text{rgb}}^{Y_j}}|^2] + \frac{(\theta_2^2 - 8(\theta_2 - 1)^2) E_i^{x_i} [|\epsilon^{R_\theta^{Y_j}}|^2]}{L^2 (2\theta_3^2 + 2(1 - \theta_3)^2) \Delta t} \right. \\
& + \left. \frac{(\theta_2^2 - 8(\theta_2 - 1)^2) E_i^{x_i} [|\epsilon^{R_{\text{rgb}}^{Y_j}}|^2]}{L^2 (2\theta_3^2 + 2(1 - \theta_3)^2) \Delta t} + \frac{4E_i^{x_i} [|\epsilon^{R_\theta^{Z_j}}|^2]}{\Delta t} + 4\Delta t \theta_2^2 E_i^{x_i} [|\epsilon^{R_{\text{rgb}}^{Z_j}}|^2] \right).
\end{aligned}$$

The regression error R_{xgb}^Z and R_{xgb}^Y are given in (17) and (27), from which one can deduce e.g.,

$|R_{\text{xgb}}^{Y_j}|^2 \leq |2(\text{Var}_j^y + \hat{\mathcal{L}}_{\min}(\hat{q}_j^y))|^2 := (\text{Var}_j^y)^2$. Similarly, for $\frac{|R_{\text{xgb}}^{Y_j}|^2}{\Delta t}$ and $\Delta t |R_{\text{xgb}}^{Z_j}|^2$ we obtain $\frac{N_T(\text{Var}_j^y)^2}{T}$ and $\frac{T(\text{Var}_j^z)^2}{N_T}$, respectively. Finally, with the known conditions and bounds of the local errors mentioned above we complete the proof. \square

Note that one can straightforwardly obtain

$$E_0^{x_0} \left[|\epsilon^{Y_i}|^2 + \frac{9\Delta t}{16} |\epsilon^{Z_i}|^2 \right] \leq Q(\Delta t)^4 + \tilde{Q} \sum_{i=1}^{N_T} \left(\frac{N_T(\text{Var}_j^y)^2}{T} + \frac{T(\text{Var}_j^z)^2}{N_T} \right),$$

when $\theta_1 = \theta_2 = \theta_3 = 1/2$ provided that $E_{N_T-1}^{x_{N_T-1}} [|\epsilon^{Z_{N_T}}|^4] \sim \mathcal{O}((\Delta t)^4)$ and $E_{N_T-1}^{x_{N_T-1}} [|\epsilon^{Y_{N_T}}|^4] \sim \mathcal{O}((\Delta t)^4)$.

5 Numerical experiments

In this section we use some numerical examples to show the accuracy of our methods for solving the high-dimensional (≥ 100 dim) BSDEs. As already introduced above, N_T and M are the total discrete time steps and sampling size, respectively. For all the examples, we consider an equidistant time grid and perform 10 Picard iterations. We ran the algorithms 10 times independently and take average value of absolute error, whereas the different seeds are used for each simulation. Numerical experiments were performed with an Intel(R) Core(TM) i5-8500 CPU @ 3.00GHz and 15 GB RAM.

5.1 The less challenging problems

If the values of the driver function f are almost constant or behave linearly along $\mathbb{X}_t = (X_t, Y_t, Z_t)$, in particular when $dX_t = dW_t$, i.e., a standard BSDE, very well approximations (\hat{Y}_0, \hat{Z}_0) , can be reached by averaging the samples at T generated with x_0 , i.e., by using the Monte-Carlo estimation. A fine time-discretization and regression are not really necessary. If g is differentiable, according to Scheme 1 we use

$$\hat{Z}_0 \approx \frac{1}{M} \sum_{\mathcal{M}=1}^M \left[\frac{2}{T} \hat{y}_{N_T, \mathcal{M}} W_{N_T, \mathcal{M}} + f(T, \hat{x}_{N_T, \mathcal{M}}, \hat{y}_{N_T, \mathcal{M}}, \hat{z}_{N_T, \mathcal{M}}) W_{N_T, \mathcal{M}} - \hat{z}_{N_T, \mathcal{M}} \right], \quad (32)$$

$$\hat{Y}_0 \approx \frac{1}{M} \sum_{\mathcal{M}=1}^M \left[\hat{y}_{N_T, \mathcal{M}} + \frac{T}{2} f(T, \hat{x}_{N_T, \mathcal{M}}, \hat{y}_{N_T, \mathcal{M}}, \hat{z}_{N_T, \mathcal{M}}) \right] + \frac{T}{2} f(0, x_0, \hat{Y}_0, \hat{Z}_0), \quad (33)$$

where $\hat{y}_{N_T, \mathcal{M}} = g(\hat{x}_{N_T, \mathcal{M}})$, $\hat{z}_{N_T, \mathcal{M}} = g_x(\hat{x}_{N_T, \mathcal{M}})$. Similarly, if g is not differentiable, one can average according to Scheme 2.

Example 1 We consider firstly a BSDE with quadratically growing derivatives derived in [Gobet and Turkedjiev, 2015], whose explicit solution is known. A modified version of that BSDE in 100-dimensional case is analyzed numerically in [E. et al., 2017], and given by

$$-dY_t = \underbrace{\|Z\|_{\mathbb{R}^{1 \times d}}^2 - \|\nabla \psi(t, W_t)\|_{\mathbb{R}^d}^2 - (\partial_t + \frac{1}{2} \Delta) \psi(t, W_t)}_{=f} dt - Z_t dW_t$$

with the analytical solution

$$\begin{cases} Y_t = \psi(t, W_t) = \sin\left((T - t + \frac{1}{d} \|W_t\|_{\mathbb{R}^d}^2)^\alpha\right), \\ Z_t = 2\alpha W_t^\top \cos\left((T - t + \frac{1}{d} \|W_t\|_{\mathbb{R}^d}^2)^\alpha\right) (T - t + \frac{1}{d} \|W_t\|_{\mathbb{R}^d}^2)^{\alpha-1}, \end{cases}$$

where $\alpha \in (0, 1/2]$, we let $\alpha = 0.4$. We observe that the driver f behaves almost linearly, see $f(T, \hat{x}_{N_T, \mathcal{M}}, \hat{y}_{N_T, \mathcal{M}}, \hat{z}_{N_T, \mathcal{M}})$ displayed in Figure 1. This is to say that we should be able use (32) and (33). We test that with different values for T and d and report our results in Table

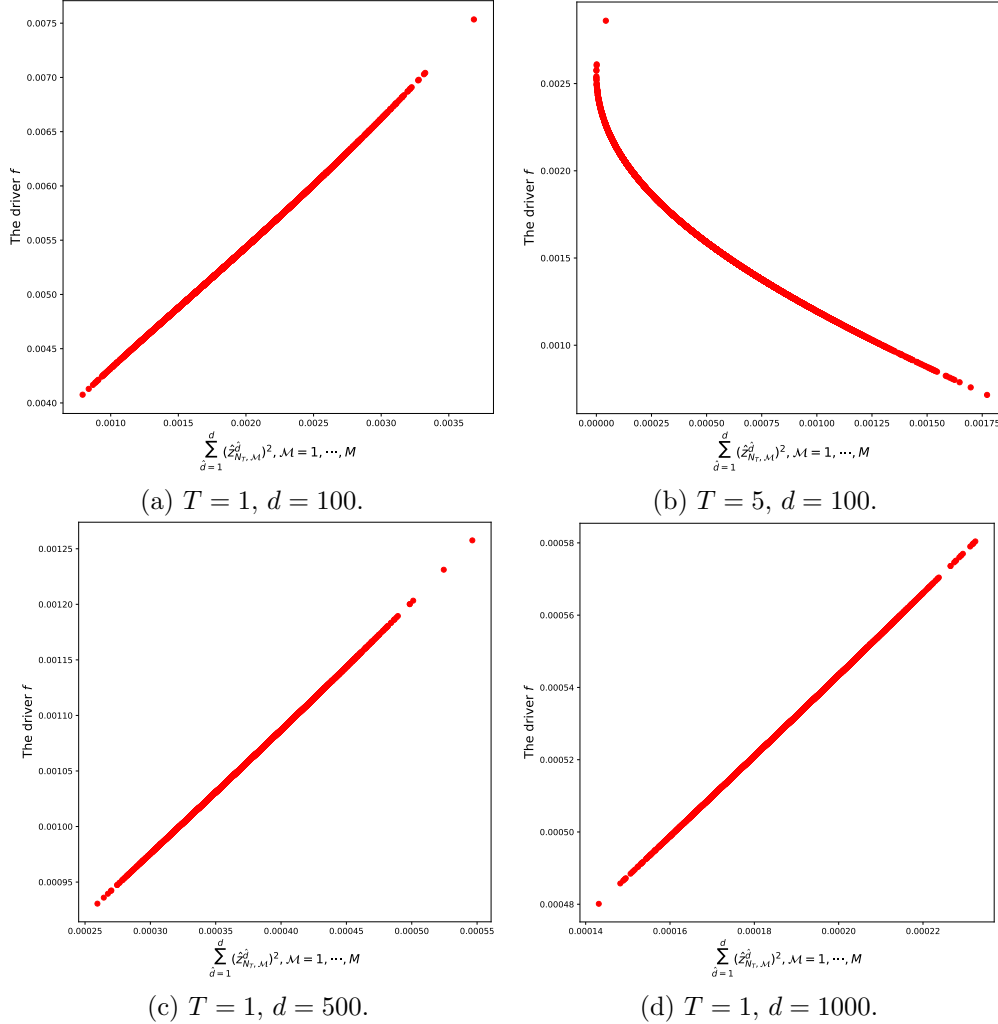


Figure 1: The samples of $f(T, X, Y, Z)$ for the samples of $\|Z\|_{\mathbb{R}^{1 \times d}}^2$ using the different values of d, T for Example 1.

1, and the average runtime of each run (in seconds) is provided as well. In high-dimensional case we have $\hat{\mathbf{Z}}_0 = (\hat{Z}_0^1, \hat{Z}_0^2, \dots, \hat{Z}_0^d)$, let $\hat{Y}_{0,k}$ and $\hat{\mathbf{Z}}_{0,k}$ denote the result on the k -th run of the algorithm, $k = 1, \dots, 10$, while (Y_0, \mathbf{Z}_0) is used for the exact solution or reference value. In our tests we consider average of the absolute errors, i.e., $error_y := \frac{1}{10} \sum_{k=1}^{10} |Y_0 - \hat{Y}_{0,k}|$ and $error_z := \frac{1}{10} \sum_{k=1}^{10} \frac{\sum_{\hat{d}=1}^d |Z_0^{\hat{d}} - \hat{Z}_{0,k}^{\hat{d}}|}{\hat{d}}$, as well as the empirical standard deviations $\sqrt{\frac{1}{9} \sum_{k=1}^{10} |\hat{Y}_{0,k} - \hat{Y}_0|^2}$ and $\sqrt{\frac{1}{9} \sum_{k=1}^{10} \left| \frac{\sum_{\hat{d}=1}^d \hat{Z}_{0,k}^{\hat{d}}}{\hat{d}} - \hat{Z}_0 \right|^2}$ with $\hat{Y}_0 = \frac{1}{10} \sum_{k=1}^{10} \hat{Y}_{0,k}$, $\hat{Z}_0 = \frac{1}{10} \sum_{k=1}^{10} \frac{\sum_{\hat{d}=1}^d \hat{Z}_{0,k}^{\hat{d}}}{\hat{d}}$. We see that the approximations are very impressive.

d	Theoretical solution	$M = 10000$ $error_y$ (Std. dev.) $error_z$ (Std. dev.) avg. runtime	$M = 20000$ $error_y$ (Std. dev.) $error_z$ (Std. dev.) avg. runtime	$M = 50000$ $error_y$ (Std. dev.) $error_z$ (Std. dev.) avg. runtime	$M = 100000$ $error_y$ (Std. dev.) $error_z$ (Std. dev.) avg. runtime
100	0.84147 $\mathbf{0}_d$	0.01475(0.00177) 0.01381(0.00093) 0.67	0.00712(0.00131) 0.00957(0.00091) 1.43	0.00280(0.00049) 0.00596(0.00048) 3.72	0.00139(0.00023) 0.00428(0.00029) 7.39
100	0.96859 $\mathbf{0}_d$	0.01959(0.00238) 0.01123(0.00076) 0.69	0.00950(0.00167) 0.00777(0.00073) 1.49	0.00371(0.00056) 0.00484(0.00039) 3.76	0.00188(0.00029) 0.00347(0.00023) 7.26
100	0.99982 $\mathbf{0}_d$	0.02092(0.00258) 0.00947(0.00062) 0.69	0.01017(0.00170) 0.00654(0.00061) 1.47	0.00394(0.00053) 0.00407(0.00033) 3.73	0.00204(0.00031) 0.00292(0.00019) 7.22
100	0.98553 $\mathbf{0}_d$	0.02039(0.00257) 0.00808(0.00054) 0.69	0.00994(0.00159) 0.00557(0.00052) 1.47	0.00383(0.00047) 0.00347(0.00029) 3.79	0.00202(0.00031) 0.00248(0.00016) 7.28
100	0.94511 $\mathbf{0}_d$	0.01883(0.00245) 0.00694(0.00045) 0.67	0.00921(0.00143) 0.00478(0.00045) 1.47	0.00353(0.00044) 0.00297(0.00025) 3.74	0.00190(0.00030) 0.00213(0.00014) 7.21
500	0.84147 $\mathbf{0}_d$	0.07103(0.00412) 0.01347(0.00040) 12.65	0.03465(0.00162) 0.00941(0.00021) 25.60	0.01426(0.00080) 0.00605(0.00018) 62.33	0.00704(0.00027) 0.00424(0.00008) 115.49
1000	0.84147 $\mathbf{0}_d$	0.14018(0.00629) 0.01336(0.00031) 46.06	0.07058(0.00249) 0.00945(0.00017) 89.93	0.02788(0.00097) 0.00597(0.00010) 218.29	0.01406(0.00026) 0.00423(0.00005) 433.45

Table 1: Numerical simulation using the method (32) and (33) for Example 1.

Example 2 Another high-dimensional example considered in the recent literature is the time-dependent reaction-diffusion-type equation

$$-dY_t = \min \left\{ 1, \left[Y_t - \kappa - 1 - \sin \left(\zeta \sum_{\hat{d}=1}^d W_t^{\hat{d}} \right) \exp \left(\frac{\zeta^2 d(t-T)}{2} \right) \right]^2 \right\} dt - Z_t dW_t$$

with the analytical solution

$$\begin{cases} Y_t = 1 + \kappa + \sin \left(\zeta \sum_{\hat{d}=1}^d W_t^{\hat{d}} \right) \exp \left(\frac{\zeta^2 d(t-T)}{2} \right), \\ Z_t = \zeta \cos \left(\zeta \sum_{\hat{d}=1}^d W_t^{\hat{d}} \right) \exp \left(\frac{\zeta^2 d(t-T)}{2} \right) \mathbf{1}_d, \end{cases}$$

which is oscillating. This example has been numerically analyzed in [Gobet and Turkedjiev, 2017] for $d = 2$, and in [E. et al., 2017] for $d = 100$. In our test we find that driver function gives very small values (up to 10^{-31}), see Figure (2), i.e., (32) and (33) can be used. Let $\kappa = \frac{7}{10}$, $\zeta = \frac{1}{\sqrt{d}}$, we report our results in Table 2.

5.2 General nonlinear high-dimensional problems

In our methods, the most important thing is to find the right values for the XGBoost hyperparameters to prevent overfitting and underfitting. In principle, one can run *GridSearchCV* to find best values of the hyperparameters, however, this is quite time consuming. Therefore, in our experiments we tune the parameters separately with the following remarks.

- In our test the results are not really sensitive with respect to the maximum depth of a tree, we fix thus \tilde{d} to be 2 for less computational cost in all the following examples.

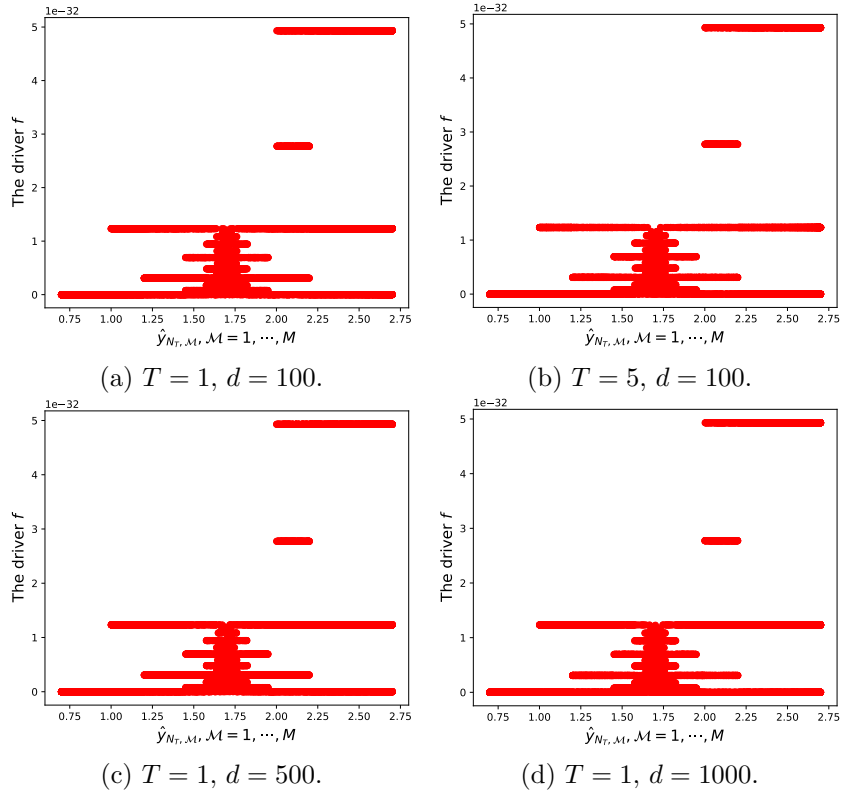


Figure 2: The samples of $f(T, X, Y, Z)$ for the samples Y using the different values of d, T for Example 2.

d	Theoretical solution Y_0 Z_0	$M = 10000$ $error_y$ (Std. dev.) $error_z$ (Std. dev.) avg. runtime	$M = 20000$ $error_y$ (Std. dev.) $error_z$ (Std. dev.) avg. runtime	$M = 50000$ $error_y$ (Std. dev.) $error_z$ (Std. dev.) avg. runtime	$M = 100000$ $error_y$ (Std. dev.) $error_z$ (Std. dev.) avg. runtime
100	1.7	0.00724(0.00875)	0.00419(0.00569)	0.00243(0.00309)	0.00176(0.00222)
1	0.06065 $\mathbf{1}_d$	0.00381(0.00459) 0.14	0.00213(0.00262) 0.32	0.00144(0.00176) 0.80	0.00091(0.00120) 1.66
100	1.7	0.00629(0.00769)	0.00425(0.00579)	0.00215(0.00266)	0.00167(0.00205)
2	0.03679 $\mathbf{1}_d$	0.00269(0.00295) 0.15	0.00150(0.00185) 0.33	0.00101(0.00125) 0.85	0.00071(0.00092) 1.67
100	1.7	0.00499(0.00682)	0.00405(0.00545)	0.00157(0.00210)	0.00169(0.00195)
3	0.02231 $\mathbf{1}_d$	0.00324(0.00192) 0.17	0.00144(0.00139) 0.35	0.00080(0.00104) 0.87	0.00065(0.00079) 1.67
100	1.7	0.00538(0.00677)	0.00377(0.00502)	0.00151(0.00182)	0.00177(0.00206)
4	0.01353 $\mathbf{1}_d$	0.00508(0.00147) 0.17	0.00196(0.00104) 0.34	0.00072(0.00085) 0.87	0.00056(0.00068) 1.68
100	1.7	0.00557(0.00706)	0.00345(0.00465)	0.00157(0.00185)	0.00185(0.00219)
5	0.00821 $\mathbf{1}_d$	0.00670(0.00129) 0.17	0.00339(0.00084) 0.37	0.00098(0.00059) 0.89	0.00045(0.00054) 1.69
500	1.7	0.00537(0.00739)	0.00383(0.00447)	0.00243(0.00301)	0.00189(0.00220)
1	0.02712 $\mathbf{1}_d$	0.00921(0.00103) 2.72	0.00359(0.00096) 5.52	0.00083(0.00088) 13.72	0.00047(0.00053) 27.10
1000	1.7	0.00623(0.00765)	0.00444(0.00539)	0.00266(0.00299)	0.00187(0.00234)
1	0.01918 $\mathbf{1}_d$	0.01341(0.00081) 10.17	0.00680(0.00060) 20.40	0.00179(0.00047) 50.94	0.00041(0.00043) 101.17

Table 2: Numerical simulation using the method (32) and (33) for Example 2.

- The datasets are splitted into train and test sets with a ratio of 75 : 25.
- We find that the most important parameters are the learning rate and the number of trees, namely K . In our test we can obtain promising results with any values of learning rate in the set of $\{0.01, 0.1, 0.2, \dots, 0.9, 0.99\}$ by adjusting a proper value of K . We denote the number of trees in individual XGBoost regressor at each time step for computing $Z_i^{\Delta t}$ and $Y_i^{\Delta t}$ by $K_{i,z}$ and $K_{i,y}$, $i = 0, \dots, N_T - 1$, respectively. In principle, we can adjust values of $K_{i,z}$ and $K_{i,y}$, i.e., at each time step. However, this is quite time consuming and thus maybe not realistic. Fortunately, we observe the learning curves for $K_{i,z}$ and $K_{i,y}$ behave quite similarly for different time step and Δt . Therefore, for all the time steps we consider K_z and K_y for computing Z - and Y - component, respectively. In Example 3 and 4 we fix the learning rate to be 0.9 for a faster computation, and choose the proper numbers of trees, namely K_z and K_y by comparing the training and test MSEs. For the challenging problems, i.e., Example 5 and 6 we fix the learning rate to be 0.1 and then correspondingly select proper values for K_z and K_y .
- For all other parameters we use the default values, e.g., $\lambda = 1$ and $\gamma = 0$.

For each example we perform 10 independent runs. We denote the approximations with XGBoost regressions by $(Y_0^{\Delta t}, \mathbf{Z}_0^{\Delta t})$ with $\mathbf{Z}_0^{\Delta t} = (Z_0^{\Delta t,1}, Z_0^{\Delta t,2}, \dots, Z_0^{\Delta t,d})$. For the Y -component we define the error and standard deviation as: $error_y := \frac{1}{10} \sum_{k=1}^{10} |Y_0 - Y_{0,k}^{\Delta t}|$ and $\sqrt{\frac{1}{9} \sum_{k=1}^{10} |Y_{0,k}^{\Delta t} - Y_0^{\Delta t}|^2}$ with $Y_0^{\Delta t} = \frac{1}{10} \sum_{k=1}^{10} Y_{0,k}^{\Delta t}$. Furthermore, for the Z -component we consider $error_z := \frac{1}{10} \sum_{k=1}^{10} \frac{\sum_{\hat{d}=1}^d |Z_{0,k}^{\hat{d}} - Z_{0,k}^{\Delta t, \hat{d}}|}{d}$ and $\sqrt{\frac{1}{9} \sum_{k=1}^{10} \left| \frac{\sum_{\hat{d}=1}^d Z_{0,k}^{\Delta t, \hat{d}}}{d} - \bar{Z}_0^{\Delta t} \right|^2}$ with $\bar{Z}_0^{\Delta t} = \frac{1}{10} \sum_{k=1}^{10} \frac{\sum_{\hat{d}=1}^d Z_{0,k}^{\Delta t, \hat{d}}}{d}$.

Example 3 To test our Scheme 2 we consider a pricing problem of an European option in a financial market with different interest rate for borrowing and lending to hedge the option. This pricing problem is analyzed in [Bergman, 1995], used as a standard nonlinear (high-dimensional) example in the many works, see e.g., [Bender et al., 2017, E. et al., 2017, E. et al., 2019, Gobet et al., 2005, Kapllani and Teng, 2020, Teng, 2019], and given by

$$\begin{cases} dS_t &= \mu S_t dt + \sigma S_t dW_t, \\ -dY_t &= -R^l Y_t - \frac{\mu - R^l}{\sigma} \sum_{\hat{d}=1}^d Z_t^{\hat{d}} + (R^b - R^l) \max\left(0, \frac{1}{\sigma} \sum_{\hat{d}=1}^d Z_t^{\hat{d}} - Y_t\right) dt - Z_t dW_t, \\ Y_T &= \max\left(\max_{\hat{d}=1, \dots, d}(S_T^{\hat{d}}) - K_1, 0\right) - 2 \max\left(\max_{\hat{d}=1, \dots, d}(S_T^{\hat{d}}) - K_2, 0\right) \end{cases}$$

where $\sigma > 0$, $\mu \in \mathbb{R}$, R^b, R^l are different interest rates and K_1, K_2 are strikes. Since Z_{N_T} is not analytically available in this example, we choose Scheme 2. The parameter values are set as: $T = 0.5$, $\mu = 0.06$, $\sigma = 0.02$, $R^l = 0.04$, $R^b = 0.06$, $K_1 = 120$ and $K_2 = 150$, for which the reference price $Y_0 = 21.2988$ is computed using the multilevel Monte Carlo with 7 Picard iterations [E. et al., 2019]. As mentioned above, we set the learning rate to be 0.9 and $\tilde{d} = 2$ for a faster computation, and tune separately to choose the value of K_z and K_y . We show the XGBoost model for Y with learning curves in Figure 3. In Figure 3(a) we see that overfitting occurs for a large value of K_y . We set thus $K_y = 20$ by observing the learning curves in Figure 3(b), which are the enlargement of the curves in Figure 3(a) until $K_y = 100$. Similarly, the value of K_z can be tuned as well, we use $K_z = 20$ in this example.

The numerical results are reported in Table 3. Note that the same reference price is used to compare the deep learning-based numerical methods for high-dimensional BSDEs in [E. et al., 2017] (Table 3), which has achieved a relative error of 0.0039 in a runtime of 566 seconds. From Table

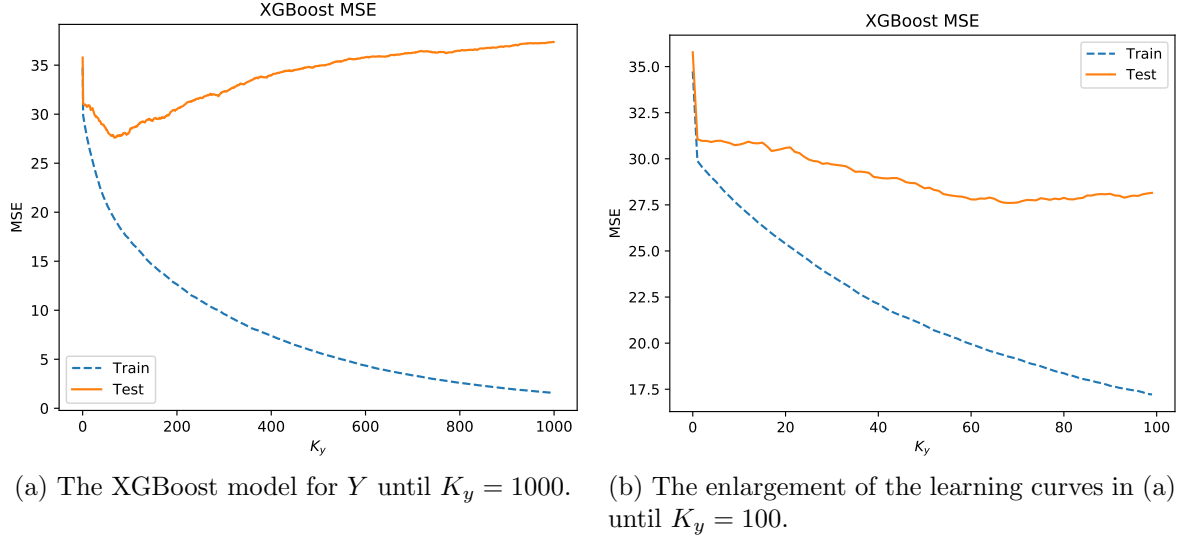


Figure 3: The MSEs of the XGBoost models in Scheme 2 for Example 3 for different numbers of trees, $N_T = 10$, $M = 10000$ and the learning rate is 0.9.

$d = 100$ $T = 0.5$ N_T	Ref. value computed with [E. et al., 2019] Y_0	$M = 10000$ $error_y$ (Std. dev.) avg. runtime	$M = 20000$ $error_y$ (Std. dev.) avg. runtime	$M = 50000$ $error_y$ (Std. dev.) avg. runtime	$M = 100000$ $error_y$ (Std. dev.) avg. runtime
10	21.2988	0.13725(0.13335) 9.10	0.13911(0.09088) 19.37	0.12952(0.06001) 54.06	0.18669(0.04351) 131.17
20	21.2988	0.20207(0.21176) 25.03	0.14609(0.16716) 51.73	0.05542(0.03960) 139.14	0.08281(0.01219) 324.49
30	21.2988	0.33619(0.43693) 40.94	0.14689(0.15127) 84.17	0.04741(0.05735) 224.13	0.04096(0.05090) 519.47

Table 3: Numerical simulation using Scheme 2 for Example 3.

$T = 0.3, N_T = 10$		$M = 2000$	$M = 5000$
d	Ref. value	$error_y$ (Std. dev.) avg. runtime	$error_y$ (Std. dev.) avg. runtime
10	0.89060	0.00279(0.00342) 0.19	0.00175(0.00233) 0.33
50	1.01830	0.00141(0.00187) 0.45	0.00076(0.00076) 1.18
100	1.04510	0.00265(0.00147) 0.85	0.00098(0.00113) 2.21
200	1.06220	0.00101(0.00130) 1.69	0.00074(0.00097) 4.31
300	1.07217	0.00247(0.00171) 2.53	0.00075(0.00044) 6.74
500	1.08124	0.00134(0.00110) 4.37	0.00071(0.00034) 11.79
1000	1.09100	0.00111(0.00142) 9.25	0.00051(0.00103) 25.33
5000	1.10691	0.00162(0.00086) 69.51	0.00174(0.00012) 129.90
10000	1.11402	0.00049(0.00087) 151.89	0.00037(0.00017) 670.24

Table 4: Numerical simulation using Scheme 1 for Example 4.

3 one see that the relative errors 0.00222 and 0.00192 can be achieved in runtime 224.13 and 519.47, respectively.

Example 4 In [Beck et al., 2019a], several examples have been numerically analyzed up to 10000 dimensions. Depending on complexity of the solution structure, the computational expenses are widely different, where the least computational effort is shown for computing the Allen-Cahn equation

$$\begin{cases} dX_t = \sigma dW_t, \\ -dY_t = (Y_t - Y_t^3) dt - Z_t dW_t, \\ Y_T = \arctan\left(\max_{\hat{d} \in \{1, 2, \dots, d\}} X_T^{\hat{d}}\right). \end{cases}$$

In this example, one has a cubic nonlinearity, and Z_T can be analytically calculated as $\left(0, \dots, \frac{1}{1+(X_T^{d_m})^2}, \dots, 0\right)$, where d_m denotes the index of maximum value. This is to say that we can use Scheme 1, for a comparative purpose we select parameter values as those in [Beck et al., 2019a]: $T = 0.3$, $\sigma = \sqrt{2}$ and $N_T = 10$. For the XGBoost hyperparameters we use the same values as those in Example 3. In Table 4 we present the numerical results for different values for d and M . We see that substantially less data are required for very well approximations in this example, and we obtain a better accuracy than that achieved in [Beck et al., 2019a] for less computational cost.

Example 5 To test our Scheme 1 exhaustively, we consider the Burgers-type equation

$$\begin{cases} dX_t = \sigma dW_t, \\ -dY_t = \left(Y_t - \frac{2+d}{2d}\right) \left(\sum_{\hat{d}=1}^d Z_t^{\hat{d}}\right) dt - Z_t dW_t, \end{cases}$$

with the analytic solution

$$\begin{cases} Y_t &= \frac{\exp\left(t + \frac{1}{d} \sum_{\hat{d}=1}^d X_t^{\hat{d}}\right)}{1 + \exp\left(t + \frac{1}{d} \sum_{\hat{d}=1}^d X_t^{\hat{d}}\right)}, \\ Z_t &= \frac{\sigma}{d} \frac{\exp\left(t + \frac{1}{d} \sum_{\hat{d}=1}^d X_t^{\hat{d}}\right)}{\left(1 + \exp\left(t + \frac{1}{d} \sum_{\hat{d}=1}^d X_t^{\hat{d}}\right)\right)^2} \mathbf{1}_d. \end{cases}$$

This example has been analyzed in [Chassagneux, 2014] for $d = 3$, $T = 1$ and $\sigma = 1$, and in [E. et al., 2019] for $d = 100$, $T = 0.5$, $\sigma = 0.25$ as well as in [E. et al., 2017] for $d = 20$, $T = 1$, $\sigma = \frac{d}{\sqrt{2}}$ and $d = 50$, $T = 0.2$, $\sigma = \frac{d}{\sqrt{2}}$. This problem in high-dimensional case is computationally challenging, the deep-learning based algorithm in [E. et al., 2017] seems diverges for $d = 100$, $T = 0.5$, $\sigma = \frac{d}{\sqrt{2}}$ (at least based on our attempts). Furthermore, the approximations of Z in the case of $d = 100$ are not given in [E. et al., 2019] and [E. et al., 2017].

Here, we solve this problem for $d = 100$, $T = 0.5$, $\sigma = \frac{d}{\sqrt{2}}$ numerically using Scheme 1. We display the MSEs of the XGBoost models for K_z and K_y on the training and test datasets in a time step in Figure 4, where $N_T = 10$, $M = 10000$. From Figure 4, it looks like that the right

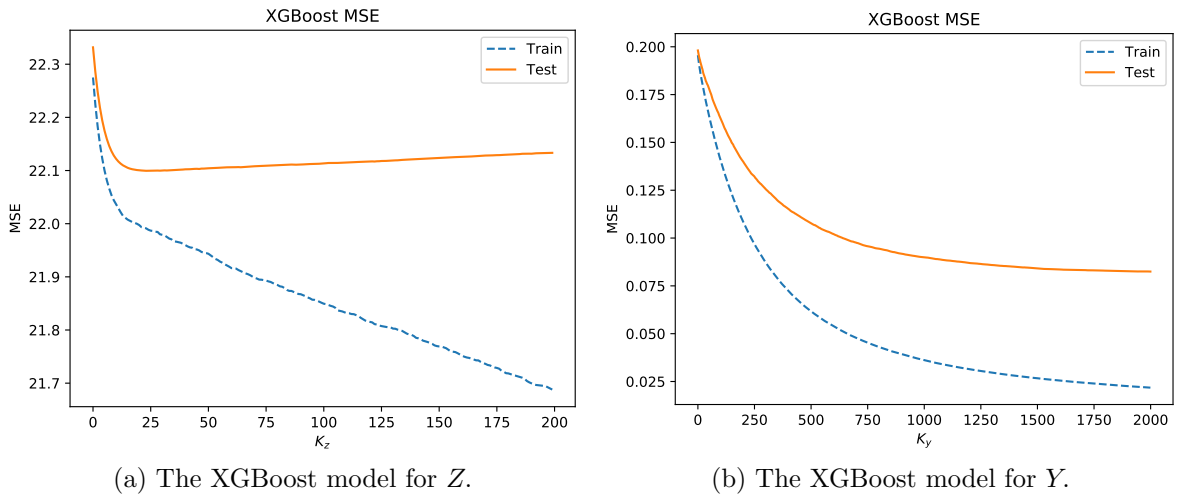


Figure 4: The MSEs of the XGBoost models in Scheme 1 for Example 5 for different numbers of trees, $N_T = 10$, $M = 10000$ and the learning rate is 0.1.

values of K_z and K_y are around 6, we thus let $K = 6$ in this example. Note that the training error for Z can be further reduced (near zero) for a large value of K_z , however, the overfitting becomes thus more severe. Finally, we present our approximations in Table 5 for different values of M, N_T . We see that the numerical results are surprisingly very good, it looks like that one needs a larger value of M to balance the discretization error for computing Z than Y .

Example 6 (A challenging problem) To further test our proposed Scheme 1 we consider a BSDE with an unbounded and complex structure solution, which has been analyzed in [Chassagneux et al., 2021, Huré et al., 2020] and reads

$$\begin{cases} dX_t &= \frac{1}{\sqrt{d}} \mathbf{I}_d dW_t, \\ -dY_t &= \left(1 + \frac{T-t}{2d}\right) A(X_t) + B(X_t) + C \cos\left(\sum_{\hat{d}=1}^d \hat{d} Z^{\hat{d}}\right) dt - Z_t dW_t, \end{cases}$$

with

$$A(x) = \frac{1}{d} \sum_{\hat{d}=1}^d \sin(x^{\hat{d}}) \mathbf{1}_{\{x^{\hat{d}} < 0\}}, \quad B(x) = \frac{1}{d} \sum_{\hat{d}=1}^d x^{\hat{d}} \mathbf{1}_{\{x^{\hat{d}} \geq 0\}}, \quad C = \frac{(d+1)(2d+1)}{12},$$

$d = 100$ $T = 0.5$	Theoretical solution	$M = 10000$ $error_y$ (Std. dev.) $error_z$ (Std. dev.) avg. runtime	$M = 20000$ $error_y$ (Std. dev.) $error_z$ (Std. dev.) avg. runtime	$M = 50000$ $error_y$ (Std. dev.) $error_z$ (Std. dev.) avg. runtime	$M = 100000$ $error_y$ (Std. dev.) $error_z$ (Std. dev.) avg. runtime
N_T	Y_0 Z_0				
10	0.5 0.17678 $\mathbf{1}_d$	0.05486(0.03434) 0.00601(0.00412) 10.66	0.05570(0.02464) 0.00529(0.00505) 22.23	0.05545(0.01359) 0.00460(0.00244) 59.58	0.05203(0.01430) 0.00454(0.00135) 152.96
20	0.5 0.17678 $\mathbf{1}_d$	0.01625(0.00038) 0.00641(0.00881) 27.11	0.01629(0.00019) 0.00560(0.00629) 55.67	0.01650(0.00010) 0.00454(0.00381) 146.40	0.01640(0.00009) 0.00387(0.00235) 369.11
30	0.5 0.17678 $\mathbf{1}_d$	0.00712(0.00010) 0.00785(0.00494) 43.55	0.00712(0.00005) 0.00526(0.00509) 88.39	0.00714(0.00005) 0.00519(0.00259) 234.21	0.00713(0.00003) 0.00424(0.00289) 583.45

Table 5: Numerical simulation using Scheme 1 for Example 5.

and the analytic solution

$$Y_t = \frac{T-t}{d} \sum_{\hat{d}=1}^d \left(\sin(X_t^{\hat{d}}) \mathbb{1}_{\{X_t^{\hat{d}} < 0\}} + X_t^{\hat{d}} \mathbb{1}_{\{X_t^{\hat{d}} \geq 0\}} \right) + \cos \left(\sum_{\hat{d}=1}^d \hat{d} Z_{\hat{d}} \right).$$

In Table 6 we report firstly our approximations for the different values of M , N_T when $d = 1, 2, 5$. Our proposed scheme works very well for the challenging problem. Note that the reported values of K_z and K_y in Table 6 are optional. For example, we display the MSEs of the XGBoost models for K_z and K_y on the training and test datasets in a time step in Figure 5 for $d = 1$, from which we roughly choose $K_z = 8$ and $K_y = 100$. In our tests, the almost same results can be obtained with values of K_z in $\{2, 3, \dots, 25\}$ and K_y in $\{10, 11, \dots, 200\}$.

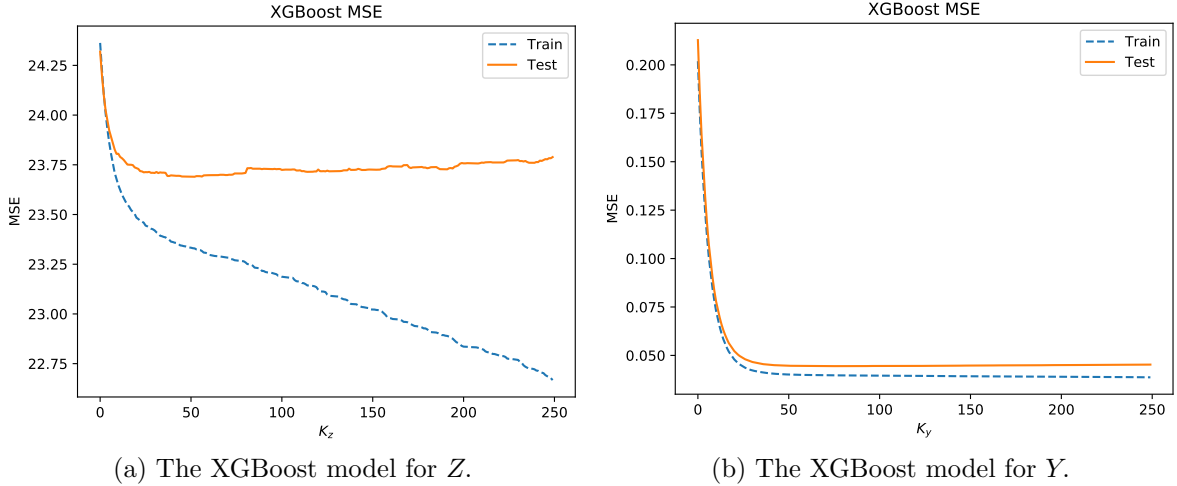


Figure 5: The MSEs of the XGBoost models in Scheme 1 for Example 6 for different numbers of trees, $N_T = 10$, $M = 10000$, $d = 1$ and the learning rate is 0.1.

As indicated in [Chassagneux et al., 2021, Huré et al., 2020], the deep learning algorithm [Han et al., 2017] fails when $d \geq 3$. Furthermore, the two backward deep learning schemes of [Huré et al., 2020] and deep learning schemes with sparse grids of [Chassagneux et al., 2021] fails when $d \geq 8$. We refer to Table 5 in [Chassagneux et al., 2021] for detailed comparisons. In Table 7 we show that our scheme works well even for $d = 50$. Note that we need to set $N_T = 400$ for $d = 50$ to obtain a good approximation, and our scheme shall work well also for a higher

$T = 1$	$M = 10000$ $error_y$ (Std. dev.) avg. runtime	$M = 50000$ $error_y$ (Std. dev.) avg. runtime	$M = 100000$ $error_y$ (Std. dev.) avg. runtime	$M = 200000$ $error_y$ (Std. dev.) avg. runtime
N_T	$d = 1, Y_0 = 1.3776, K_z = 10, K_y = 100$			
10	0.00371(0.00501) 0.72	0.00153(0.00188) 2.94	0.00096(0.00112) 5.80	0.00118(0.00169) 11.62
20	0.00565(0.00649) 1.51	0.00127(0.00121) 6.25	0.00173(0.00220) 12.36	0.00087(0.00128) 24.77
30	0.00526(0.00598) 2.31	0.00112(0.00170) 9.54	0.00159(0.00191) 18.86	0.00134(0.00141) 37.98
N_T	$d = 2, Y_0 = 0.5707, K_z = 8, K_y = 150$			
10	0.00893(0.01154) 1.10	0.00505(0.00622) 4.69	0.00278(0.00359) 9.21	0.00258(0.00337) 18.69
20	0.01156(0.01370) 2.31	0.00376(0.00437) 10.01	0.00317(0.00386) 19.81	0.00327(0.00340) 40.05
30	0.01167(0.01772) 3.52	0.00558(0.00607) 15.32	0.00325(0.00425) 30.34	0.00177(0.00252) 61.56
N_T	$d = 5, Y_0 = 0.8466, K_z = 2, K_y = 150$			
10	0.02626(0.03105) 1.68	0.01533(0.01038) 7.91	0.01191(0.00681) 16.02	0.00917(0.00545) 32.79
20	0.01854(0.02541) 3.58	0.01101(0.01310) 17.27	0.00537(0.00761) 34.72	0.00398(0.00489) 70.96
30	0.02439(0.03115) 5.48	0.00687(0.00947) 26.49	0.00718(0.01015) 53.30	0.00452(0.00437) 108.78

Table 6: Numerical simulation using Scheme 1 for Example 6.

$T = 1$ $M = 20000$	Theoretical solution	Numerical approximation	$error_y$ (Std. dev.)	$K_z = K_y$	avg. runtime
d N_T	Y_0	$Y_0^{\Delta t}$			
8 20	1.16032	1.16830	0.01047(0.00931)	12	5.47
10 20	-0.21489	-0.21517	0.02435(0.03030)	40	14.19
20 30	0.25904	0.2555	0.02838(0.03492)	16	32.55
50 400	-0.47055	-0.47437	0.00667(0.00778)	10	1805.75

Table 7: The numerical approximation of Y_0 using Scheme 1 for Example 6 when $T = 1$.

dimension if Δt is sufficiently small. However, a higher dimension ($d > 50$) is not considered here due to the long computational time. The results can be further improved with a larger value of simple size.

6 Conclusion

In this work, we have proposed the XGBoost regression-based algorithms for numerically solving high-dimensional nonlinear BSDEs. We show how to use the XGBoost regression to approximate the conditional expectations arising by discretizing the time-integrands using the general theta-discretization method. The time complexity and error analysis have been provided as well. We have performed several numerical experiments for different types of BSDEs including 10000-dimensional nonlinear problem. Our numerical results are quite promising and indicate that the proposed algorithms are very attractive to solve high-dimensional nonlinear BSDEs.

Acknowledgment

The author gratefully acknowledges in-depth discussions with Prof. Dr. Hanno Gottschalk from the University of Wuppertal.

The author would like to thank Lorenc Kapllani for his assistance.

References

- [Beck et al., 2019a] Beck, C., Becker, S., Cheridito, P., Jentzen, A., and Neufeld, A. (2019a). Deep splitting method for parabolic pdes. *Available on webpage at <https://arxiv.org/pdf/1907.03452v1.pdf>*.
- [Beck et al., 2019b] Beck, C., E, W., and Jentzen, A. (2019b). Machine learning approximation algorithms for high-dimensional fully nonlinear partial differential equations and second-order backward stochastic differential equations. *J. Nonlinear Sci.*, 29(4):1563–1619.
- [Beck et al., 2020] Beck, C., Hutzenthaler, M., Jentzen, A., and Kuckuck, B. (2020). An overview on deep learning-based approximation methods for partial differential equations. *Available on webpage at <https://arxiv.org/pdf/2012.12348v1.pdf>*.
- [Becker et al., 2020] Becker, S., Braunwarth, R., Hutzenthaler, M., Jentzen, A., and von Wurstemberger, P. (2020). Numerical simulations for full history recursive multilevel picard approximations for systems of high-dimensional partial differential equations. *Commun. Comput. Phys.*, 28(5):2109–2318.
- [Bender et al., 2017] Bender, C., Schweizer, N., and Zhuo, J. (2017). A primal-dual algorithm for bsdes. *Math. Financ.*, 27(3):866–901.
- [Bergman, 1995] Bergman, Y. Z. (1995). Option pricing with differential interest rates. *Rev. Financ. Stud.*, 8(2):475–500.
- [Breiman, 2001] Breiman, L. (2001). Random forests. *Mach. Learn.*, 45(1):5–32.
- [Chassagneux, 2014] Chassagneux, J. F. (2014). Linear multistep schemes for bsdes. *SIAM J. Numer. Anal.*, 52(6):2815–2836.

- [Chassagneux et al., 2021] Chassagneux, J. F., Chen, J., Frikha, N., and Zhou, C. (2021). A learning scheme by sparse grids and Picard approximations for semilinear parabolic PDEs. *available on webpage at <https://arxiv.org/pdf/2102.12051v1.pdf>*.
- [Chen and Guestrin, 2016] Chen, T. and Guestrin, C. (2016). XGBoost: a scalable tree boosting system. In *Proceedings of the 22nd ACM SIGKDD international conference on knowledge discovery and data mining*. San Francisco California, USA.
- [Dorogush et al., 2018] Dorogush, A., Ershov, V., and Gulin, A. (2018). CatBoost: gradient boosting with categorical features support. *Available on webpage at <https://arxiv.org/pdf/1810.11363v1.pdf>*.
- [E. et al., 2017] E., W., Han, J., and Jentzen, A. (2017). Deep learning-based numerical methods for high-dimensional parabolic partial differential equations and backward stochastic differential equations. *Commun. Math. Stat.*, 5(4).
- [E. et al., 2019] E., W., Hutzenthaler, M., Jentzen, A., and Kruse, T. (2019). On multilevel picard numerical approximations for high-dimensional nonlinear parabolic partial differential equations and high-dimensional nonlinear backward stochastic differential equations. *J. Sci. Comput.*
- [Friedman, 2002] Friedman, J. (2002). Stochastic gradient boosting. *Comput. Stat. Data Anal.*, 38(4):367–378.
- [Friedman and Popescu, 2003] Friedman, J. H. and Popescu, B. E. (2003). Importance sampled learning ensembles.
- [Germain et al., 2020] Germain, M., Pham, H., and Warin, X. (2020). Deep backward multistep schemes for nonlinear pdes and approximation error analysis. *Available on webpage at <https://arxiv.org/pdf/2006.01496v1.pdf>*.
- [Germain et al., 2021] Germain, M., Pham, H., and Warin, X. (2021). Neural networks-based algorithms for stochastic control and pdes in finance. *Available on webpage at <https://arxiv.org/abs/2101.08068v2>*.
- [Gobet et al., 2005] Gobet, E., Lemor, J. P., and Warin, X. (2005). A regression-based monte carlo method to solve backward stochastic differential equations. *Ann. Appl. Probab.*, 15:2172–2202.
- [Gobet and Turkedjiev, 2015] Gobet, E. and Turkedjiev, P. (2015). Linear regression mdp scheme for discrete backward stochastic differential equations under general conditions. *Math. Comput.*, 85(299):1359–1391.
- [Gobet and Turkedjiev, 2017] Gobet, E. and Turkedjiev, P. (2017). Adaptive importance sampling in least-squares monte carlo algorithms for backward stochastic differential equations. *Stochastic Process. Appl.*, 127(4).
- [Han et al., 2017] Han, J., Jentzen, A., and E, W. (2017). Solving high-dimensional partial differential equations using deep learning. In *Proceedings of the National Academy of Sciences*, volume 115 (34). USA.
- [Huré et al., 2020] Huré, C., Pham, H., and Warin, X. (2020). Deep backward schemes for high-dimensional nonlinear pdes. *Math. Comput.*, 89:1547–1579.

- [Hutzenthaler et al., 2020] Hutzenthaler, M., Jentzen, A., Kruse, T., and Nguyen, T. (2020). Multilevel picard approximations of high-dimensional semilinear second-order pdes with lipschitz nonlinearities. *Available on webpage at <https://arxiv.org/pdf/2009.02484.pdf>.*
- [Hutzenthaler and Kruse, 2020] Hutzenthaler, M. and Kruse, T. (2020). Multilevel picard approximations of high-dimensional semilinear parabolic differential equations with gradient-dependent nonlinearities. *SIAM J. Numer. Anal.*, 58(2):929–961.
- [Ji et al., 2020] Ji, S., Peng, S., Peng, Y., and Zhang, X. (2020). Three algorithms for solving high-dimensional fully coupled fbsdes through deep learning. *IEEE Intell. Syst.*, 35(3).
- [Kapllani and Teng, 2020] Kapllani, L. and Teng, L. (2020). Deep learning algorithms for solving high dimensional nonlinear backward stochastic differential equations. *submitted, available on webpage at <https://arxiv.org/pdf/2010.01319.pdf>.*
- [Karoui et al., 1997a] Karoui, N. E., Kapoudjan, C., Pardoux, E., Peng, S., and Quenez, M. C. (1997a). Reflected solutions of backward stochastic differential equations and related obstacle problems for pdes. *Ann. Probab.*, 25:702–737.
- [Karoui et al., 1997b] Karoui, N. E., Peng, S., and Quenez, M. C. (1997b). Backward stochastic differential equations in finance. *Math. Finance*, 7(1):1–71.
- [Ke et al., 2017] Ke, G., Meng, Q., Finley, T., Wang, T., Chen, W., Ma, W., Ye, Q., and Liu, T. (2017). LightGBM: a highly efficient gradient boosting decision tree. In *Proceedings of the 31st international conference on neural information processing system*. Curran Associates Inc., Long Beach, CA, USA.
- [Ma and Zhang, 2005] Ma, J. and Zhang, J. (2005). Representations and regularities for solutions to bsdes with reflections. *Stoch. Proc. Appl.*, 115:539–569.
- [Pardoux and Peng, 1990] Pardoux, E. and Peng, S. (1990). Adapted solution of a backward stochastic differential equations. *System and Control Letters*, 14:55–61.
- [Pardoux and Peng, 1992] Pardoux, E. and Peng, S. (1992). Backward stochastic differential equation and quasilinear parabolic partial differential equations. *Lectures Notes in CSI.*, 176:200–217.
- [Peng, 1991] Peng, S. (1991). Probabilistic interpretation for systems of quasilinear parabolic partial differential equations. *Stochastics and Stochastic Reports*, 37(1–2):61–74.
- [Pham et al., 2021] Pham, H., Warin, X., and Germain, M. (2021). Neural networks-based backward scheme for fully nonlinear pdes. *SN PDE*, 2(1).
- [Ruijter and Oosterlee, 2015] Ruijter, M. J. and Oosterlee, C. W. (2015). A fourier cosine method for an efficient computation of solutions to bsdes. *SIAM J. Sci. Comput.*, 37(2):A859–A889.
- [Teng, 2019] Teng, L. (2019). A review of tree-based approaches to solve forward-backward stochastic differential equations. *J. Comput. Finance (forthcoming)*.
- [Teng et al., 2020] Teng, L., Lapitckii, A., and Günther, M. (2020). A multi-step scheme based on cubic spline for solving backward stochastic differential equations. *Appl. Numer. Math.*, 150.
- [Teng and Zhao, 2021] Teng, L. and Zhao, W. (2021). High-order combined multi-step scheme for solving forward backward stochastic differential equations. *J. Sci. Comput.*, 87(81).

- [Yang et al., 2017] Yang, L., Jie, Y., and Zhao, W. (2017). Convergence error estimates of the crank-nicolson scheme for solving decoupled fbsdes. *Sci. China Math.*, 60:923–948.
- [Zhao et al., 2006] Zhao, W., Chen, L., and Peng, S. (2006). A new kind of accurate numerical method for backward stochastic differential equations. *SIAM J. Sci. Comput.*, 28(4):1563–1581.
- [Zhao et al., 2014] Zhao, W., Fu, Y., and Zhou, T. (2014). New kinds of high-order multistep schemes for coupled forward backward stochastic differential equations. *SIAM J. Sci. Comput.*, 36(4):A1731–A1751.
- [Zhao et al., 2013] Zhao, W., Li, Y., and Ju, L. (2013). Error estimates of the crank-nicolson scheme for solving backward stochastic differential equations. *Int. J. Numer. Anal. Model.*, 10(4):876–898.
- [Zhao et al., 2012] Zhao, W., Li, Y., and Zhang, G. (2012). A generalized θ -scheme for solving backward stochastic differential equations. *Discrete Cont. Dyn-B.*, 17(5):1585–1603.
- [Zhao et al., 2009] Zhao, W., Wang, J., and Peng, S. (2009). Error estimates of the θ -scheme for backward stochastic differential equations. *Discrete Contin. Dyn. Syst. Ser. B*, 12:905–924.